

Numerical Simulation of Foundation Pit Dewatering Using Horizontal Seepage Reducing Body

Jianxiu Wang (✉ wang_jianxiu@163.com)

Tongji University

Yanxia Long

Tongji University

Yu Zhao

Tongji University

Weiqiang Pan

Shanghai Tunnel Engineering Company Co.,Ltd

Jianxun Qu

Shanghai Tunnel Engineering Company Co.,Ltd

Hanmei Wang

Shanghai Institute of Geological Survey

Yujin Shi

Shanghai Institute of Geological Survey

Xiaotian Liu

Tongji University

Research Article

Keywords: confined aquifer, foundation pit dewatering, vertical curtain, horizontal seepage reducing body (HSRB), three-dimensional numerical simulation, seepage mode

Posted Date: September 29th, 2021

DOI: <https://doi.org/10.21203/rs.3.rs-936569/v1>

License:  This work is licensed under a Creative Commons Attribution 4.0 International License.

[Read Full License](#)

Version of Record: A version of this preprint was published at Scientific Reports on January 26th, 2022. See the published version at <https://doi.org/10.1038/s41598-022-05348-y>.

1 **Numerical simulation of foundation pit dewatering using horizontal**
2 **seepage reducing body**

3 Jianxiu Wang^{1,2,*}, Yanxia Long¹, Yu Zhao¹, Xiaotian Liu¹, Weiqiang Pan³, Jianxun Qu³,
4 Hanmei Wang⁴, Yujin Shi⁴

5 ¹College of Civil Engineering, Tongji University, Shanghai, 200092, China

6 ²Key Laboratory of Geotechnical and Underground Engineering of Ministry of Education, Tongji
7 University, Shanghai, China

8 ³Shanghai Tunnel Engineering Company Co.,Ltd., Shanghai 200082, China

9 ⁴Shanghai Institute of Geological Survey, Shanghai 200093, China

10
11 **Corresponding author:** *Jianxiu Wang, Department of Geotechnical Engineering, Tongji
12 University, Shanghai 200092, China; wang_jianxiu@163.com; Tel: +86-13916185056,
13 +86 21 65983036; Fax: +86 21 659851011

23 **Abstract:** Groundwater level has to be lowered during deep excavation. A vertical curtain is
24 usually adopted to control the drawdown both inside and outside a foundation pit in a built-up area.
25 However, the cost and working difficulty increases substantially with the increasing depth of vertical
26 curtains. In the manuscript, a kind of man-made horizontal seepage reducing body (HSRB) was
27 introduced to shorten the vertical curtain depth and control drawdown. With the No. 4 shaft
28 foundation pit of Guangyuan Project, Shanghai as background, HSRB was proposed in foundation
29 pit dewatering. Microbially induced carbonate precipitation grouting technology was recommended
30 to form an environment-friendly HSRB. Numerical method was used to simulate and understand
31 the influence of position, thickness, and hydraulic conductivity of HSRB on groundwater level. The
32 non-separated HSRB was better than the separate HSRB. Decreasing HSRB hydraulic conductivity
33 was better than increasing HSRB depth. Four seepage modes are summarized considering vertical
34 curtain penetration conditions into multi-aquifer, and the fifth seepage mode was formed for vertical
35 curtain using man-made HSRB, which can be referred by similar engineering.

36 **Keywords:** confined aquifer, foundation pit dewatering, vertical curtain, horizontal seepage
37 reducing body (HSRB), three-dimensional numerical simulation, seepage mode

38
39
40
41
42
43
44

45 **1 Introduction**

46 Coastal cities are often developed in economic because of convenient transportation. Urbanization
47 develops quickly. Underground space is developed to serve the development of the city. In the aspect
48 of engineering geology, engineering hydro-geology is important for a coastal city. Multi aquifer and
49 multi aquitard are often encountered during underground exploitation. How to deal with the multi-
50 aquifer is significant for a deep excavation. Meanwhile, how to control the environment influence
51 of lowering ground water level is also important. The excavation depth continuously increased under
52 the urbanization demand, the required drawdown is increasing correspondingly. The contradiction
53 between the increasing drawdown and strict requirements of surrounding land subsidence, together
54 with groundwater resource protection, is also expanding. The majority of the accidents in foundation
55 pit are concerned with groundwater. How to control groundwater level effectively during excavation
56 has become a research hotspot (**Cong et al., 2009; Wang et al., 2010; You et al., 2017; Cui, 2017;**
57 **Estanislao et al., 2017; Zhang et al., 2019; Li et al., 2021**). The improper control of groundwater
58 in excavation and construction processes often leads to large ground deformation (**Caldhead et al.,**
59 **2011; Xu et al., 2012; Pujes et al., 2017**), damage to surrounding buildings (**Song et al., 2014; Tan**
60 **et al., 2018**), quicksand and gushing (**Zheng et al., 2016; Wu et al, 2018, 2019**), and other
61 engineering hazards. Field monitoring has indicated that the pumping and depressurization of
62 confined water are the main factors causing ground settlement in foundation pit engineering (**Chen**
63 **et al., 2009; Ye et al., 2009**). The influence range reaches 10 to 15 times of the excavation depth
64 (**Gong et al., 2008**). Therefore, groundwater control in excavation is necessary to ensure the safety
65 both for foundation pit and environment.

66 At present, curtain cutoff, pumping, and recharging are widely used in groundwater control of a

67 foundation pit (**Fig. 1**). Pumping is generally used and curtain is currently utilized to achieve
68 foundation pit dewatering (**Ha et al., 2018; Wang et al., 2016, 2017**). Vertical curtain is usually
69 used to cut off aquifers, decrease aquifer discharge section, change seepage direction, prolong
70 seepage path. Some studies have evaluated the dewatering effect of the insertion depth of vertical
71 curtain (**Feng et al., 2013; Zhao et al., 2020; Li et al., 2017; Wu et al., 2019**), pumping rate (**Li et**
72 **al., 2020**), hydraulic conductivity, and distance between pumping well and vertical curtain (**Wang**
73 **et al., 2016, 2017**). Wang et al. (**2010**) analyzed the mode and mechanism of the wall–well
74 interaction, four patterns including fully enclosed, flush, partially enclosed, and fully exposed types
75 are defined. The depth of vertical curtain penetrating into aquifer influence drawdown obviously.
76 The interaction between vertical curtain and pumping well should be considered in foundation pit
77 dewatering (i.e., wall–well interaction) (**Wu et al., 2019**). The application of the wall–well
78 interaction in different projects was also summarized (**Wang et al., 2009, 2010, 2013, 2014**).
79 However, the verticality of curtain, such as diaphragm wall, is difficult to be controlled precisely
80 when the depth of vertical curtain is too large. If the verticality is not controlled in a certain value,
81 the foot of two adjacent diaphragm wall splits leading to water leakage, which is dangerous for
82 groundwater control. The vertical curtain cannot cut off aquifers and cannot meet the strict
83 settlement control requirements of the surrounding environment when the aquifer is too deep. This
84 type of deep confined aquifers has led to the use of horizontal curtain (**Liu, 2010**). However,
85 horizontal curtain cannot avoid local leakage owing to complex hydrogeological conditions and
86 construction quality. Local leakage points result in water inrush.

87 In the manuscript, a kind of man-made horizontal aquiclude with lower permeability was introduced
88 in the dewatering system with vertical curtain. A kind of man-made horizontal seepage reducing

89 body (HSRB) was proposed. With the No. 4 shaft foundation pit of the Guangyuan Project, Shanghai
90 as background, HSRB was suggested to combine with vertical curtain to control groundwater
91 drawdown. Microbially induced carbonate precipitation (MICP) grouting technology was suggested
92 to form the HSRB. Finite difference method (FDM) was used to simulate the working mechanism
93 of HSRB. The position, thickness, and hydraulic conductivity of HSRB were analyzed, which can
94 be referred by similar projects.

95 **2 Material and methods**

96 **2.1 Project overview**

97 The No. 4 shaft foundation pit (**Fig. 2**) of Guangyuan Project in Pudong New District, Shanghai is
98 located on Jihui Road of Gaoyan Institute, 97.1 m away from the West 220 kV high-voltage iron
99 tower, 12 m away from the east substation, and 8.5 m nearest to a two-story pump house. The
100 surrounding environment of the shaft was complicated. The foundation pit is a 55 m × 50 m
101 rectangular in plane. The designed ground elevation is 4.5 m, while the pit excavation depth is 39.6
102 m. The foundation pit bottom was located in the silty clay of layer ⑤. The enclosure retaining
103 system composed of diaphragm wall, outer trench cutting re-mixing deep wall (TRD), and inner
104 support. Diaphragm wall was also used as vertical curtain for dewatering.

105 The 150-m depth layers of the site was composed of the Quaternary Holocene to Middle Pleistocene
106 sedimentary strata. The strata are divided into 10 main engineering geological layers (**Fig. 2(b)**).

107 The layer ⑤₁ and above layers were generalized as shallow soil layers.

108 The aquifers consisted of phreatic aquifer (shallow soil layers), micro confined aquifer (layer ⑤),
109 confined aquifer I (layer ⑦), confined aquifer II (layer ⑨), and confined aquifer III (layer ⑪).

110 The recommended hydraulic conductivity for each layer based on laboratory and in-site pumping

111 test are shown in **Table 1**.

112 The foundation pit bottom was mainly located in clayey soil. Dewatering schemes for each aquifer
 113 under the pit were arranged as shown in **Table 2**.

114 An MICP man-made HSRB was suggested besides the vertical curtain consisted by diaphragm wall
 115 and TRD to reduce the influence on surrounding environment. MICP grouting technology was
 116 suggested to form the HSRB using *bacillus pasteurella* and cementing fluid (CaCl₂ solution, urea
 117 solution).

118 2.2 Numerical modeling

119 The hydrogeological conceptual model was translated into a mathematical model. The accuracy of
 120 the model was verified via model identification and verification. A three-dimensional unsteady flow
 121 continuity equation was established in anisotropic porous media:

$$\begin{cases}
 \frac{\partial}{\partial x} \left(k_{xx} \frac{\partial h}{\partial x} \right) + \frac{\partial}{\partial y} \left(k_{yy} \frac{\partial h}{\partial y} \right) + \frac{\partial}{\partial z} \left(k_{zz} \frac{\partial h}{\partial z} \right) - W = \frac{E}{T} \frac{\partial h}{\partial t} \dots\dots\dots(x, y, z) \in \Omega \\
 h(x, y, z, t) \Big|_{t=0} = h_0(x, y, z) \dots\dots\dots(x, y, z) \in \Omega \\
 h(x, y, z, t) \Big|_{\Gamma_1} = h_1(x, y, z) \dots\dots\dots(x, y, z) \in \Gamma_1 \\
 h(x, y, z, t) \Big|_{\Gamma_2} = h_2(x, y, z) \dots\dots\dots(x, y, z) \in \Gamma_2
 \end{cases} \quad (1)$$

123 where $E = \begin{cases} S & \text{Confined aquifer} \\ S_y & \text{Diving aquifer} \end{cases}$; $T = \begin{cases} M & \text{Confined aquifer} \\ B & \text{Diving aquifer} \end{cases}$; $S_s = \frac{S}{M}$; S is water

124 storage coefficient, S_y is water supply, S_s is water storage rate (1/m); M is unit thickness of the

125 confined aquifer (m); B is saturated thickness of groundwater in the phreatic aquifer unit body

126 (m); k_{xx}, k_{yy}, k_{zz} are the anisotropic principal direction hydraulic conductivities (m/d); h is

127 head value of point (x, y, z) at time t (m); W is source and exchange items (1/d); h_0 is

128 initial head value of the calculation domain (m); h_1 is value of the water head around the first

129 boundary (m); h_2 is water head value of the first boundary of the foundation pit (m); t is time

130 (d); and Ω is computational domain; Γ_1 is Dirichlet boundary; Γ_2 is Neumann boundary.

131 With the shaft foundation pit as center, a 2000 m \times 2000 m and 150 m deep modeling range was
132 selected. The range was generalized into a 3D heterogeneous, horizontally isotropic, and unstable
133 groundwater seepage system. The model was divided into 11 layers according to soil layer
134 distribution. The ground elevation was taken as + 4.5 m (**Fig. 3**). The outer boundary was defined
135 as constant water head boundary, and the bottom was set as impermeable boundary. Model hierarchy
136 and its parameters are shown in **Table 1**.

137 For the shaft foundation pit was too deep, the confined aquifer II which was seldom concerned
138 previously had to be lowered. Although double vertical curtains were adopted, the layer ⑨ was
139 not cut off. MICP HSRB was suggested to control the drawdown which was discussed in another
140 manuscript*. According to laboratory results, the hydraulic conductivity of the layer ⑨ was
141 decreased from 2.1×10^{-3} cm/s to 1.9×10^{-4} cm/s using the MICP technology.

142 In working conditions, the influence of the position, thickness, and permeability of the horizontal
143 curtain on the foundation pit dewatering was designed. The working conditions of numerical
144 simulation is shown in **Table 3**.

145 FDM was used to solve the problem. The conjugate gradient method (PCG) was chosen to
146 simultaneously solve the algebraic equations. Groundwater level changes inside and outside the
147 foundation pit were simulated.

148 **3 Results**

149 **3.1 Results without HSRB**

150 In case 1, four wells were used to pump water simultaneously, and the pumping rate of the four
151 wells was 2950 m³/d. After continuous pumping for 6 days, the dynamic water level of the fourth

152 pumping well in layer ⑧₂₂ of the pit decreased by 9.0 m, and the minimum drawdown in the
153 foundation pit was 5.56 m, which met the requirements of the foundation pit anti-gushing
154 calculation, and the drawdown in the layer ⑧₂₂ was 5.5 m (**Fig. 4(a)**). The change of the minimum
155 water level decrease with time in the pit is shown in **Fig. 5**. At this time, water level in the range of
156 600 m of layer ⑧₂₂ outside the pit decreased by 4.70 m to 0.83 m. When the dewatering of layer
157 ⑧₂₂ met the drawdown requirement (i.e., continuous pumping for 6 days), the drawdown of four
158 wells in layer ⑨ in the pit was 12.0 m, and the minimum water level drawdown of layer ⑨ in the
159 pit was 5.3 m, which met the requirement of 2.3 m drawdown of layer ⑨ in the foundation pit anti-
160 gushing calculation (**Fig. 4(b)**). The variation of the minimum water level drawdown with time in
161 the pit is shown in **Fig. 5(a)**. At this time, the water level within 600 m of layer ⑨ outside the pit
162 decreased by 4.70 m to 0.82 m, as shown in **Fig.5(b)**.

163 As shown in **Fig. 5**, under the simultaneous action of four pumping wells, the water level of the
164 deep foundation pit of the No. 4 working well decreased rapidly in the first day, reaching 5.3 m.
165 However, the design drawdown meeting the anti-gushing calculation can be achieved on the sixth
166 day owing to the large permeability of the second confined aquifer in Shanghai and the large
167 pumping rate of the foundation pit. As shown in **Fig. 6**, the drawdown of the water level outside the
168 foundation pit of layer ⑧₂₂ and layer ⑨ coincided with the distance, and the change of the
169 drawdown curve can be divided into three areas. (1) Within the range of 0 to 150 m, the drawdown
170 gradient with the distance was large, and the change of water level was large. (2) Within the range
171 of 150 m to 300 m, the gradient of the drawdown with the distance began to decrease, and the change
172 of water level was slow and gradually transited to the slow area. Beyond the range of 300 m, the
173 drawdown gradient with distance was small, and the change of water level was small as well.

174 **3.2 Influence of HSRB position on dewatering**

175 Before forming a horizontal curtain by using the MICP technology, the depth of the horizontal
176 curtain setting should be determined. This set the top plate of the horizontal curtain at the
177 equilibrium position of the water and soil pressure after the excavation of the foundation pit. The
178 calculation formula is as follows:

179
$$\sum \gamma_i h_i \geq \gamma_s \gamma_w H, \quad (2)$$

180 where γ_i is weight of each layer of soil (kN/m³); h_i is thickness of each layer (m); H is pressure
181 head height at the horizontal curtain (m); γ_w is water severity (kN/m³), take 10 kN/m³; and γ_s is
182 safety coefficient, take 1.05.

183 The buried depth of the horizontal curtain was 82 m, as calculated using formula (2).

184 According to the calculation results of working conditions 2 to 7, combined with the comparative
185 analysis of the calculation results of condition 1, the influence of HSRB at different positions on
186 deep foundation pit dewatering was studied. The thickness of HSRB was 4 m, and the hydraulic
187 conductivity was 5×10^{-3} cm/s. According to the different positions of the horizontal curtain, the
188 combination forms of the three-dimensional curtain were classified into inner-wrapping, flush, and
189 separated types, as shown in **Table 4**.

190 Four pumping wells (i.e., 4y9-1 to 4y9-4) were used to pump water simultaneously in conditions 2
191 to 7, and the pumping rate of the four wells was 2950 m³/d. According to the calculation results, the
192 time required for the drawdown of the water level in the pit to reach the design drawdown can be
193 obtained, as shown in **Fig. 7**. When the buried depths of HSRB were 80, 82, 84, and 86 m. That is,
194 when the horizontal curtain was not separated from the three-dimensional curtain, the time required
195 to reach the water level in the pit to reach the designed drawdown level of the foundation pit anti-

196 gushing calculation was substantially shortened compared with that without horizontal curtain,
197 which was only approximately 28.8 min, and only 0.4% of that without horizontal curtain. For
198 several working conditions of the non-separated three-dimensional curtain, the position and depth
199 of horizontal curtain had minimal influence on the dewatering time of the deep foundation pit.
200 When the buried depths of the horizontal curtain were 88, 90, and 92 m (i.e., HSRB and vertical
201 curtain were separated and combined to form separate three-dimensional curtain), the times required
202 to reach the design drawdown were 0.35, 0.55, and 0.8 d, respectively. Compared with the non-
203 separated three-dimensional curtain, the time to reach the design drawdown was increased.
204 However, the time to reach the design drawdown was also significantly shorter than that without
205 HSRB, which was only approximately 10% of that without HSRB. With the deepening of the buried
206 depth of the horizontal curtain, the time required for the foundation pit dewatering to reach the
207 design drawdown increased correspondingly.

208 Therefore, from the perspective of dewatering time, the effect of setting HSRB on the design
209 drawdown of the foundation pit dewatering was significant, and the effect of the non-separation
210 three-dimensional curtain was better than that of the separation three-dimensional curtain. The work
211 efficiency of setting horizontal curtain was evidently higher than that without HSRB. In practical
212 engineering, the construction period was substantially reduced, construction efficiency was
213 considerably improved, construction nodes can be completed in advance, and good social and
214 economic benefits will be achieved.

215 To significantly compare the influence of the different types of three-dimensional curtain on deep
216 foundation pit dewatering, the non-separation and separation three-dimensional curtain were studied
217 separately. Working conditions 2 to 4 were calculated to study the influence of the position of the

218 non-separating horizontal curtain on the three-dimensional curtain–well group system. The
219 minimum drawdown of the water levels in the pit of layers ⑧₂₂ and ⑨ are shown in **Figs. 7(a)**
220 and **7(b)**, respectively. The drawdown time curve under the working conditions of 82, 84, and 86 m
221 of the horizontal curtain had minimal difference. After 28.8 min of pumping well operation, the
222 drawdown of the water level in the pit reached 5.6m of the design requirement.

223 Working conditions 4 to 6 were calculated to study the influence of the position of the separated
224 horizontal curtain on the three-dimensional curtain–well group system, working conditions 4 to 6
225 were calculated. The minimum drawdown of the water levels in the pit of layers ⑧₂₂ and ⑨ are
226 shown in **Figs. 7(c)** and **7(d)**, respectively. The time required to reach the design drawdown in the
227 pit increased with the deepening of HSRB. Before reaching the design drawdown, the deeper HSRB
228 was buried, the smaller the minimum drawdown in the foundation pit under the corresponding
229 working conditions.

230 During the excavation of the deep foundation pit in Shanghai, the main purpose of extracting
231 groundwater from the deep second confined aquifer was to reduce the water head pressure at the
232 bottom of the pit and avoid the occurrence of sudden gushing at the bottom of the pit. However, the
233 decrease of the groundwater level leads to an increase of the effective self-weight stress of the layer
234 below the original water level, soil consolidation, ground settlement around the foundation pit, and
235 uneven settlement, inclination, and cracking of underground pipelines and surface buildings.
236 Therefore, effective measures should be implemented to reduce or even eliminate the impact of
237 foundation pit dewatering on the surrounding environment. The setting of vertical curtain relatively
238 reduced the impact of foundation pit dewatering on the surrounding environment. However, merely
239 setting a vertical curtain may not meet the requirements for engineering with strict requirements on

240 the surrounding environment. Hence, HSRB should be added to further eliminate the settlement of
241 the pit bottom caused by foundation pit dewatering. Therefore, the influence of HSRB on
242 groundwater level outside the pit must also be referred to evaluate the effect of the different HSRB
243 position, thickness, and hydraulic conductivity on the three-dimensional curtain–well group system
244 on the deep foundation pit dewatering engineering.

245 As shown in **Figs. 8(a)** and **8(b)**, the variation law of the drawdown distance curve outside the pit
246 of layers ⑧₂₂ and ⑨ under each working condition was consistent. Meanwhile, the drawdown
247 value and drawdown trend of the water levels outside the pit of layers ⑧₂₂ and ⑨ were basically
248 the same. Therefore, this study only analyzed the drawdown variation outside the pit of layer ⑧₂₂
249 with distance. For the working condition of non-separated three-dimensional curtain, when the
250 HSRB buried depths were 82, 84, and 86 m, the drawdown distance curves of the three working
251 conditions were nearly coincidental. When the drawdown of water level in the pit reached the design
252 requirement of 5.52 m, the maximum drawdown of the water level outside the pit was 2.4 m, and
253 the drawdown of the water level outside the pit was 0.5 m when the drawdown of the water level
254 outside the pit was 150m. For the non-separated three-dimensional curtain, the position of the HSRB
255 in the three-dimensional curtain has evident minimal influence on the deep foundation pit
256 dewatering project, which can be disregarded.

257 For the working conditions of the separated curtain (i.e. when HSRB buried depths were 88, 90, and
258 92 m), the variation trend of the drawdown distance curve outside the pit under the three working
259 conditions was consistent, and the curve slope was the same. That is, the drawdown rate of the water
260 level outside the pit was the same with a decrease in distance. However, the drawdown of the water
261 level outside the pit was different with the varying positions of HSRB. The deeper the HSRB was

262 buried, the higher the drawdown of the water level outside the pit; and the greater the settlement of
263 the ground outside the pit, the greater the impact on the environment. When HSRB depth was 88 m,
264 the maximum drawdown of the water level outside the pit was 4.3 m and the maximum drawdown
265 400 m away from the pit was 0.84 m. When HSRB depth was 90 m, the maximum drawdown of the
266 water level outside the pit was 4.5 m and the maximum drawdown 450 m away from the pit was
267 0.91 m. When the HSRB depth was 92 m, the maximum drawdown of the water level outside the
268 pit was 4.6 m and the maximum drawdown 500 m away from the pit was 0.92 m.

269 In summary, for the non-separation type of three-dimensional curtain, the effects of the inner-
270 wrapped, flush, and transitional three-dimensional curtains on the deep foundation pit dewatering
271 engineering are equivalent, and they are better than the effect of the separation type three-
272 dimensional curtain. In the separated three-dimensional curtain, the closer the horizontal curtain to
273 the bottom of the vertical curtain, the better the effect. Therefore, the design form of non-separated
274 three-dimensional curtain should be adopted in practical engineering.

275 **3.3 Influence of HSRB thickness on dewatering**

276 From the analysis results of the influence of HSRB position on the three-dimensional curtain–well
277 group system, the effect of the non-separated HSRB was better than the separated horizontal curtain,
278 and the influence of the HSRB position on the dewatering effect of the internal three-dimensional
279 curtain was minimally evident. Given that the MICP technology was used to form a horizontal
280 curtain, which involved the seepage of bacteria and cementation liquids in groundwater, to avoid
281 the impact of bacteria and cementation liquids used in MICP on the surrounding environment,
282 vertical curtain was used to control the MICP bacteria and cementation liquids within the scope of
283 the vertical curtain of foundation pit. Therefore, when the buried depth of the horizontal curtain roof

284 was set at 82 m, the thickness of the MICP bacterial liquid infusion was not over 6 m, thereby
285 reducing the impact on the surrounding environment.

286 If the pumping rate of 2950 m³/d was the same as that of conditions 2 to 7, and the horizontal curtain
287 thickness was increased, then dewatering in the foundation pit rapidly reached the designed
288 drawdown. Difficulty is encountered in analyzing the relationship between the drawdown of HSRB
289 with different thickness and time. Therefore, the pumping rate of the pumping well should be
290 reasonably reduced. Designing conditions 8, 9, and 2 were compared and analyzed to evaluate the
291 influence of pumping rate of the pumping well on the dewatering of the deep foundation pit. Only
292 the pumping rate was different under the three conditions, and other conditions were the same. The
293 specific parameters are shown in **Table 5**.

294 According to the numerical simulation results, the drawdown-to-time curves of the water level in
295 the pit under three conditions of the different pumping rates are shown in **Figs. 9(a)** and **Fig. 9(b)**,
296 and the drawdown to distance curves outside the pit are shown in **Figs. 10(a)** and **10(b)**. As shown
297 in **Figs. 9(a)** and **9(b)**, when the pumping rate of the pumping well decreased from 2950 m³/d to
298 2500 m³/d, the time required for the water level in the pit to reach the design drawdown increased.
299 When pumping rate was 2950 m³/d, 28.8 min was needed to reach the design drawdown. When
300 pumping rate was 2500 m³/d, 72 min was needed to reach the design drawdown. When pumping
301 rate was 2000 m³/d, 72 min was needed to reach the design drawdown. When pumping rate was
302 2500 m³/d, 72 min was needed to reach the design drawdown. Lastly, when pumping rate was 2000
303 m³/d, 72 min was needed to reach the design drawdown.

304 As shown in **Figs. 10(a)** and **10(b)**, the drawdown value and drawdown trend of the water level
305 outside the pit of the two layers were the same. Therefore, only the variation of the drawdown of

306 the water level outside the pit of the two layers with the distance were analyzed. When pumping
307 rate was 2950 m³/d, the maximum drawdown was 2.3 m, reaching a stable drawdown of 0.48 m at
308 200 m away from the pit. When pumping rate was 2500 m³/d, the maximum drawdown was 2.5 m,
309 reaching a stable drawdown of 0.52 m at 200 m away from the pit. When pumping rate was 2000
310 m³/d, the maximum drawdown was 3.1 m, reaching a stable drawdown of 0.75 m at 300 m away
311 from the pit. With a decrease in pumping rate, the maximum drawdown of the water level outside
312 the pit increased, and the distance to reach the stable drawdown level also increased. That is, the
313 impact on the surrounding environment increased substantially.

314 In summary, different pumping rates have an impact on the effect of deep foundation pit dewatering.
315 The lower the pumping rate, the longer the time to reach the designed drawdown level and the larger
316 the drawdown and influence range of the water level outside the pit. Therefore, a high pumping rate
317 was beneficial to the deep foundation pit dewatering project, although a necessary action is to set a
318 reasonable pumping rate that considers the actual situation of the construction site.

319 To study the influence of HSRB thickness on the three-dimensional curtain–well group system, the
320 calculation of working conditions 8, 10, 11, and 12 was performed. Four pumping wells in each
321 working condition pump water at a pumping rate of 2500 m³/d. The buried depth of the horizontal
322 curtain roof was 82 m, and the horizontal curtain thicknesses in each working condition were 3, 4,
323 5, and 6 m. The three-dimensional curtain formed by the horizontal and vertical curtains was inner-
324 wrapped three-dimensional curtain, and the hydraulic conductivity was 5×10^{-3} cm/s. The specific
325 parameters are shown in **Table 6**.

326 According to the numerical simulation results, the drawdown time curves of the water level in the
327 pit under four working conditions with different thicknesses of the HSRB are shown in **Figs. 11(a)**

328 and **11(b)**. Evidently, the variation law of the drawdown time curve in the two soil layers was
329 consistent. With the increase of the HSRB thickness, minimal time was needed to achieve the design
330 drawdown. Before reaching the design drawdown, the greater the thickness of HSRB, the greater
331 the drawdown of the water level in the foundation pit. When water level in the pit reached the
332 designed drawdown in layer ⑧₂₂, drawdown in the pit in layer ⑨ can reach at least 5.4 m, which
333 can meet the design drawdown of the anti-gushing calculation in layer ⑨. Therefore, the pumping
334 time only needed to meet the drawdown requirements of the water level in layer ⑧₂₂. In case 8,
335 when HSRB thickness was 3 m and the drawdown in the pit met the design requirements, the
336 pumping well should work for approximately 0.15 d. In case 9, when HSRB thickness was 4 m and
337 the drawdown in the pit met the design requirements, the pumping well should work approximately
338 72 min. When the horizontal curtain thickness was 5 m in working condition 10 and drawdown in
339 the pit met the design requirements, the pumping well must work for approximately 36 min. When
340 HSRB thickness of working condition 11 was 6 m and drawdown in the pit met the design
341 requirements, the pumping well should work for approximately 22 min. When HSRB thickness was
342 3 m to 6 m, pumping time for the foundation pit dewatering to reach the design water level was
343 reduced by approximately 50% when the thickness was increased by 1 m. Accordingly, the pumping
344 efficiency approximately doubled.

345 The thicker the HSRB, the higher the working efficiency of the pumping well. However, with the
346 increase of thickness, the improvement range of the working efficiency of the pumping well
347 decreased. Therefore, designing a three-dimensional curtain in an actual project entails
348 comprehensive consideration of the effect and cost should be comprehensively considered to select
349 the most appropriate horizontal thickness.

350 According to the numerical simulation results, the drawdown–distance curves of the four working
351 conditions with different HSRB thicknesses are shown in **Figs. 12(a)** and **12(b)**. The drawdown
352 value and trend of the drawdown rate of water level outside the pit were the same with layers ⑧₂₂
353 and⑨. Evidently, this study only analyzed the drawdown variation of the water level outside the pit
354 with the distance in layer ⑧₂₂. The thicker the HSRB, the deeper the water level decreased at the
355 same distance outside the pit. The change trend of the drawdown–distance curve was consistent
356 under the four conditions, and the slope of the curve was the same. That is, the drawdown rate with
357 distance was the same. When HSRB thickness was 3 m, the maximum drawdown outside the pit
358 was 3.1 m, reaching a stable drawdown of 0.6 m at 350 m away from the pit. When HSRB thickness
359 was 4m, the maximum drawdown outside the pit was 2.5 m, reaching a stable drawdown of 0.52 m
360 at 250 m away from the pit. When HSRB thickness was 5 m, the maximum drawdown outside the
361 pit was 2.0 m, reaching a stable drawdown of 0.53 m at 200 m away from the pit. When HSRB
362 thickness was 6 m, the maximum drawdown outside the pit was 1.7 m, and the stable drawdown
363 was 0.51 m at 200 m away from the pit. When HSRB thickness increases from 3 m to 4 m, the lifting
364 effect was significant. Thereafter, with the increase of thickness, the curves begin to get closer with
365 the increase of thickness, and a trend of gradual coincidence was observed. That is, when the
366 horizontal curtain thickness relatively increased, increasing the horizontal curtain thickness will no
367 longer significantly improve the foundation pit dewatering effect.

368 Therefore, with an increase in HSRB thickness, the time required for the drawdown in the pit to
369 reach the design value was reduced, the maximum drawdown outside the pit was reduced, and the
370 influence range of drawdown outside the pit was reduced. When HSRB thickness was small, the
371 effect of increasing curtain thickness was considerably evident. When thickness increased to a

372 certain extent, the effect of increasing curtain thickness was minimally evident. Therefore, the effect
373 and cost should be comprehensively considered in the engineering design of three-dimensional
374 curtain, and the most appropriate horizontal curtain thickness must be selected.

375 **3.4 Influence of HSRB hydraulic conductivity on dewatering**

376 According to the analysis results of the influence of the position and thickness of the horizontal
377 seepage reducing curtain on the dewatering effect of the deep foundation pit of the three-
378 dimensional curtain-well group system, on the basis of the existing 86-m deep vertical curtain,
379 adding an HSRB with the roof buried depth of 82 m and thickness of 6 m had the best effect on the
380 control of dewatering period and the decline of the underground water level outside the pit in the
381 dewatering process of the deep foundation pit.

382 Working conditions 13 to 15 and 12 were compared and analyzed to study the influence of hydraulic
383 conductivity of HSRB on deep foundation pit dewatering. Four pumping wells under four working
384 conditions were pumped at a pumping rate of 2500 m³/d, the buried depth of HSRB roof was 82 m,
385 and HSRB thickness was 6 m. The form of the three-dimensional curtain formed by horizontal and
386 vertical curtains was inner-wrapped three-dimensional curtain. The hydraulic conductivities of
387 working conditions 13, 12, 14, and 15 were 1×10^{-2} , 5×10^{-3} , 1×10^{-4} , and 5×10^{-4} cm/s,
388 respectively, as shown in **Table 7**.

389 According to the results of the numerical simulation, drawdown–time curves of the water level in
390 the pit under four conditions with different hydraulic conductivities are shown in **Figs. 13(a)** and
391 **13(b)**, and the drawdown to distance curves outside the pit are shown in **Figs. 14(a)** and **14(b)**. As
392 shown in **Figs. 13(a)** and **Fig. 13(b)**, with a decrease in the hydraulic conductivity of the HSRB, the
393 time required for the water level in the pit to reach the design drawdown decreased. When water

394 level in the pit reached the designed drawdown of layer ⑧₂₂, the drawdown of the water level in
395 the pit of layer ⑨ can reach at least 5.5 m, which met the design drawdown of the surge calculation
396 of layer ⑨. Therefore, the pumping time only needed to meet the seepage reduction demand of
397 layer ⑧₂₂. When the hydraulic conductivity of HSRB was 1×10^{-2} cm/s, 0.20 d was needed to
398 reach the design drawdown. When the hydraulic conductivity of HSRB was 5×10^{-3} cm/s, 22 min
399 was needed to reach the design drawdown. When the hydraulic conductivity of HSRB was 1×10^{-3}
400 cm/s, the water level in the foundation pit decreased rapidly, reaching 9.3 m in 15 min. When the
401 hydraulic conductivity of HSRB was 5×10^{-4} cm/s, the drawdown of water level in the foundation
402 pit was faster than that in working condition 14, reaching 11.1 m in 15 min. When the hydraulic
403 conductivity of HSRB was below 1×10^{-3} cm/s, only 5% of the hydraulic conductivity of 1×10^{-2}
404 cm/s was needed to reach deeper drawdown. Therefore, dewatering time can be considered a
405 secondary factor, and drawdown outside the pit was mainly considered. That is, the impact of the
406 foundation pit dewatering on the environment outside the pit.

407 As shown in **Figs. 14(a)** and **(b)**, the drawdown value and drawdown trend outside the pit of the
408 two layers were the same. With a decrease in the hydraulic conductivity of HSRB, the maximum
409 drawdown of the water level outside the pit was smaller, and the influence of foundation pit
410 dewatering on the outside of the pit became smaller. Therefore, only the variation of the drawdown
411 of water level outside the pit of layer ⑧₂₂ with the distance was analyzed. When the hydraulic
412 conductivity of HSRB was 1×10^{-2} cm/s, the maximum drawdown of the water level outside the pit
413 was 3.2 m, and stable drawdown of the water level was 0.67 m at 350 m away from the pit. When
414 the hydraulic conductivity of HSRB was 5×10^{-3} cm/s, the maximum drawdown of the water level
415 outside the pit was 1.7 m, and stable drawdown of the water level was 0.48 m at 150 m away from

416 the pit. When the hydraulic conductivity of HSRB was 1×10^{-3} cm/s, the maximum drawdown of
417 the water level outside the pit was 0.93 m, and stable drawdown of the water level was 0.42 m at
418 150 m away from the pit. When the hydraulic conductivity of HSRB was 5×10^{-4} cm/s, the
419 maximum drawdown of the water level outside the pit was 0.71 m, and the stable drawdown of the
420 water level was 0.42 m at 150 m away from the pit. With a decrease in hydraulic conductivity of
421 horizontal curtain, the curves of each working condition were increasingly closer, particularly when
422 the hydraulic conductivity of HSRB was below 1×10^{-3} cm/s. Accordingly, the curves began to
423 overlap, thereby indicating that the improvement effect of lowering the hydraulic conductivity when
424 it was below 1×10^{-3} cm/s was no longer evident.

425 Therefore, with a decrease in the hydraulic conductivity of HSRB, the time required for water level
426 in the pit to reach the design drawdown was reduced, the maximum drawdown outside the pit was
427 decreased, and the impact of foundation pit dewatering outside of the pit was reduced. When the
428 hydraulic conductivity of HSRB was reduced from 1×10^{-2} cm/s to 5×10^{-3} cm/s, the improvement
429 effect was evident. However, when hydraulic conductivity of HSRB was reduced below 1×10^{-3}
430 cm/s, the improvement effect of further reduction of hydraulic conductivity on the drawdown and
431 influence range of drawdown outside the pit was no longer evident. Therefore, when using the MICP
432 technology to reduce the permeability of sand, blindly pursuing lower permeability is no longer
433 necessary.

434 **4 Discussions**

435 **4.1 Fifth foundation pit seepage modes**

436 In deep foundation pit dewatering, vertical curtains are often adopted in multi-aquifer and multi-
437 aquitard (MAMA) to control drawdown inside and outside pit. Wu et al. (2003) summarize three

438 seepage modes of foundation pit considering vertical penetration condition in MAMA. The seepage
439 mode outside curtain during portal and export dewatering for a shield machine in MAMA was
440 defined as the fourth seepage mode (Wu et al. 2010). The four seepage modes (Fig. 15) were based
441 on vertical curtain and the penetration conditions of MAMA (Wu 2003; Wang et al. 2009; Xu et
442 al. 2014; Wu et al. 2015a, f; Zhang et al. 2015b).

443 (1) Mode I (Curtain penetrating shallow aquifers and partially penetrating bottom aquitard of the
444 target aquifer of a MAMA)

445 In the mode, vertical curtain cuts off all the target aquifers (should be dewatered) of MAMA. The
446 bottom of the vertical curtain penetrated all shallow aquifers and partially penetrated the top aquitard
447 of the lowest confined aquifer that should be dewatered. The side and bottom boundaries of the
448 water flow were the cutoff wall and aquitard, respectively. Water level in the pit was lowered using
449 pumping wells within the boundaries. Three sub-modes were defined according to the dewatered
450 aquifers.

451 Mode 1-1: The excavation face located in the phreatic aquifer and underlying confined water
452 pressure satisfied anti-gushing conditions, and vacuum well point, waterway, and shallow pumping
453 well were arranged to drain the aquifers.

454 Mode 1-2: The excavation face located in the phreatic aquifer and underlying confined water
455 pressure did not satisfy anti-gushing conditions, and pumping wells were arranged to drain the
456 phreatic aquifer and lower the water level of the confined aquifer.

457 Mode 1-3: The excavation face located in the confined aquifer, the top aquitard of the shallow
458 confined aquifer was excavated, and pumping wells were arranged to drain the phreatic aquifer,
459 shallow confined aquifers, and exposed confined aquifer.

460 (2) Mode II (Curtain penetrating shallow aquifers and partially penetrating top aquitard of a
461 MAMA).

462 The vertical curtain penetrated the top aquitard of the deepest confined aquifer that should be
463 dewatered. Vertical curtain penetrated and cut off all shallow aquifers. However, no vertical curtain
464 penetrated the deepest confined aquifer that needed to lower water level. Three sub-modes were
465 defined according to the dewatered aquifer. Modes 2-1, 2-2, and 2-3 were the same as modes 1-1,
466 1-2, and 1-3 for shallow aquifers. Separated pumping wells had to be arranged in the deepest
467 confined aquifer inside or outside the pit to lower the water level. Seepage mode included the water
468 flow in shallow aquifers cut off by walls, underlying water flow in deep aquifer without cutoff walls,
469 and cross-flow between the shallow and deep aquifers.

470 (3) Mode III (Curtain penetrating shallow aquifers and partially penetrating deep target aquifers of
471 a MAMA).

472 The cut off wall penetrated the shallow MAMA aquifers and partially penetrated deep confined
473 aquifer that should be dewatered. Cut off shallow aquifers can be divided into three sub-modes
474 similar to those defined in Modes I and II. According to the depth of the cut off wall and pumping
475 well filter tubes bottom, four pumping well arrangement patterns were formed for the underlying
476 partially penetrated curtain, including the (1) entire filter tube enveloped by curtain pattern, (2) filter
477 tube partially enveloped by curtain and part of the filter tube exposed a curtain pattern, and (3) all
478 filter tube exposed curtain pattern. Nine seepage modes were combined: Mode III-1i(i=1,2,3), Mode
479 III-2j(j=1,2,3), and Mode III-3k (k=1,2,3) in curtain pattern. Water flow occurred in cut off shallow
480 aquifers and partially cut off deep aquifers, together with the leakage and crossflow between the
481 shallow and deep aquifers.

482 (4) Mode IV (Pumping outside curtain and nearby shield tunnel type).

483 When a shield machine entered or left the portal or expose working pit, dewatering was occasionally
484 necessary to control water pressure and leakage of reinforced soil. Pumping wells were arranged
485 outside the cut off wall and near the shield machine and tunnel. The cutoff wall and tunnel influenced
486 the water flow as boundaries. The dewatering type was defined as Mode IV.

487 The current four seepage modes were used widely used. However, vertical curtain may be unable
488 to effectively cut off all confined aquifers of MAMA and achieve the designed dewatering effects
489 when the confined aquifer was considerably thick or buried substantially deep. The current study
490 introduced a HSRB as man-made aquiclude to decrease hydraulic conductivity in deep confined
491 aquifer. The man-made HSRB belongs to a type of anti-seepage body formed by various
492 construction technologies at a certain depth of confined aquifers. Horizontal curtain was previously
493 used as a complete impermeable curtain, the seepage of which belongs to Mode I. Horizontal curtain
494 required advanced construction technology and cost was high. The man-made HSRB was formed
495 to improve the vertical water blocking effect rather than a water proof curtain. HSRB reduced the
496 hydraulic conductivity of aquifer soil by grouting and other techniques to weaken the hydraulic
497 connection inside and outside the pit. The conceptual model is shown in **Fig. 16**.

498 HSRB decreased the hydraulic conductivity of the soil by grouting in confined aquifer, formed an
499 HSRB with certain thickness to reduce seepage in foundation pit dewatering, increased hydraulic
500 gradient in the curtain body, and reduced outlet water pressure and effectively controlled seepage
501 flow. Compared with the complete impervious curtain, this method was economical, simple, and
502 easy to realize. Seepage occurred inside the body and bears substantial hydrodynamic force to
503 decrease the outlet water pressure.

504 According to the relative position of HSRB and vertical curtain, the combination can be divided
505 into two categories: separated and non-separated. Non-separated can be sub-divided into three types:
506 inner-wrapped, transitional, and flush.

507 (1) Mode V-1(Separated): HSRB was separated from the suspension waterproof curtain, as shown
508 in **Fig. 17(a)**. HSRB was equivalent to setting a certain area as man-made aquiclude in the aquifer
509 below the vertical curtain at certain depths. Mode was formed in the cases that the HSRB was deeper
510 than vertical curtain and formed after the vertical one.

511 (2) Mode V-2 (Inner-wrapped curtain): The HSRB was inside the vertical curtain, as shown in **Fig.**
512 **17(b)**, similar to a box that only allows a small amount of water to seep at the bottom. Given that
513 HSRB was completely within the vertical curtain range, when grouting technology was used to form
514 HSRB, vertical curtain can prevent grout from spreading into surrounding groundwater, thereby
515 reducing environmental pollution.

516 (3) Mode V-3 (Flush curtain): The top of the HSRB connected with the vertical curtain, as shown
517 in **Fig. 17(c)**. This three-dimensional curtain was approximately the same as the inner-wrapped
518 three-dimensional curtain, and both form a partially closed box with the vertical curtain. The
519 construction of this type of scheme can avoid the influence of the vertical curtain and can be realized
520 through some processes outside the pit. However, the influence of the groundwater seepage field
521 outside the pit should be considered.

522 (4) Mode V-4 (Transitional curtain): Given that the horizontal body had a certain thickness, the top
523 of the horizontal body was within the depth of the vertical curtain and the bottom plate was outside
524 the range of the vertical curtain depth. This three-dimensional curtain that transitioned from an inner
525 envelope to a level was defined as a transition three-dimensional curtain, as shown in **Fig. 17(d)**.

526 Suspended vertical curtain and HSRB were combined in foundation pit dewatering, as shown in **Fig.**
527 **18**. The HSRB was divided into full and local HSRB. Full HSRB contacted with vertical curtain to
528 form a partially closed box. The partially HSRB did not contact vertical curtain to form a non-closed
529 solid curtain.

530 When the survey data showed numerous underlying partial impermeable zones or weakly permeable
531 water bodies in the confined aquifer, these natural horizontal water-tight structures can be utilized
532 to control the design cost and construction difficulty (i.e., local horizontal curtains were set around
533 the weak water-permeable body).

534 **4.2 HSRB construction method**

535 The man-made HSRB can be considered a type of permeable horizontal curtain. At present, the
536 main forms of vertical curtain include diaphragm wall, soil mixing wall (SMW) method, cement–
537 soil mixing method, and high-pressure jet grouting method. Diaphragm wall can be used as retaining
538 structure, and widely used as vertical curtain in deep foundation pit. However, its cost was high
539 when used as curtain. The SMW method can also combine the functions of waterproof and retaining
540 structure by mixing cement slurry with the original soil and inserting an H-shaped steel. The SMW
541 method had short construction period, low environmental impact, good seepage insulation effect,
542 and relatively low cost. This method included dry and wet construction processes with short
543 construction period and low requirements for construction conditions. However, the working depth
544 of the method was limited. The high-pressure jet grouting method can combine support row piles or
545 soil nail walls to achieve waterproof and retain functions. It cut the soil mass through the cement
546 slurry ejected from the nozzle, mixing the undisturbed soil and slurry to form cement soil, and
547 hydraulic conductivity of cement–soil was considerably lower than that of the undisturbed soil mass.

548 This method was easy to construct and construction equipment was simple. However, guaranteeing
549 construction quality was difficult when the construction depth was considerably deep. Freezing
550 method has immense advantages in the construction of complex and special strata, including
551 convenient construction and recoverable engineering equipment. The deeper the excavation depth,
552 the better the freezing method. However, water cannot be pumped during the freezing period.
553 Special attention should be given to the overall stability, freezing, and thermal insulation of the
554 curtain.

555 The HSRB construction method should be selected according to engineering, geological, and
556 economic conditions. The HSRB was permeable instead of impermeable curtain, the main purpose
557 was to reduce the hydraulic conductivity of the target aquifer from 1 to 2 order of magnitude to
558 decrease the permeability of the target aquifer. Grouting method was often suggested. However, the
559 high pressure of jet cement destroyed the structure of aquifer and aquitard, and partial leakage
560 cannot be avoided. When depth was large, the connection of the different piles was difficult. This
561 study suggested the MICP grouting technology to form HSRB with grout of *bacillus pasteurilla*
562 and cementing fluid (CaCl₂ solution, urea solution), which has minimal impact on the environment.
563 The structure of the aquitard and aquifer were not destroyed.

564 The traditional materials used in the traditional horizontal curtain forming method, such as cement
565 and lime cementitious materials, caused adverse effects on the ecological environment of
566 groundwater. Moreover, traditional grouting materials have difficulty entering the sand layer with
567 small pores, such as layer ⑨ of fine sand in Shanghai. The original structure of the target aquifer
568 was destroyed in traditional technology to form a horizontal curtain. Therefore, using the MICP
569 grouting technology to form environment-friendly horizontal curtain can solve numerous limitations

570 of the traditional horizontal curtain forming method. The formation method of MICP HSRB was
571 presented in another manuscript*.

572 **5 Conclusions**

573 (1) On the bases of vertical waterproof curtain applied in foundation pit dewatering engineering,
574 HSRB was added to form a horizontal man-made aquiclude. The vertical curtain, HSRB and
575 pumping wells were designed to work together. The combination included separated and non-
576 separated types.

577 (2) For non-separation HSRB, the inner-wrapped, flush, and transitional vertical curtains were
578 equivalent. Non-separation HSRB, were better than the separation HSRB. For separated HSRB, the
579 closer to the vertical curtain bottom, the better the dewatering effect.

580 (3) The time reaching the designed drawdown, the maximum outside drawdown, and influence
581 range decreased with increasing HSRB thickness.

582 (4) When HSRB thickness was thin, increasing HSRB thickness was considerably evident. When
583 HSRB thickness was increased to a certain extent, the increasing of curtain thickness was less
584 evident. The effect and cost should be comprehensively considered, and the most appropriate HSRB
585 thickness must be selected.

586 (5) Based on the combination of vertical curtain and HSRB, the fifth seepage mode was suggested
587 for foundation pit dewatering which can be referred by similar projects.

588 **Declaration of Competing Interest**

589 The authors declared that there is no conflict of interest.

590

591 **Acknowledgements**

592 This study is sponsored by the Shanghai Municipal Science and Technology Project (18DZ1201301;
593 19DZ1200900), Key Laboratory of Land Subsidence Monitoring and Prevention, Ministry of
594 Natural Resources of the People's Republic of China (No. KLLSMP202101), Suzhou Rail Transit
595 Line 1 Co. Ltd, Xiamen Road and Bridge Group (XM2017-TZ0151; XM2017-TZ0117), China
596 Railway 15 Bureau Group Co., and IGCP Project (663-La Subsidence in Coastal cities).

597 **References**

- 598 Calderhead, A.I., Therrien, R., Rivera, A., Martela, R., Garfiasd, J., 2011. Simulating pumping-
599 induced regional land subsidence with the use of InSAR and field data in the Toluca Valley, Mexico.
600 *Adv. Water Resour.* 34, 83–97.
- 601 Cong, A.S., 2009. Discussion on seepage stability of deep foundation pit on multilayer foundation.
602 *Journal of rock mechanics and engineering*, 28 (10): 2018-2023.
- 603 Cui, Y.G., 2017. Study on water head rise of bottom side surge of foundation pit with suspended
604 curtain. *Acta geologica Sinica*, 25 (3): 699-705.
- 605 Chen, H.S., Chen, B., He, D., 2009. Risk classification of ground settlement for deep foundation pit
606 engineering in Shanghai. *Journal of underground space and engineering*, 5 (4): 829-833.
- 607 Estanislao, P., Ander, L., Jesus, C., et al., 2012. Barrier effect of underground structures on aquifers.
608 Elsevier B.V, 145-146.
- 609 Feng, X.L., Li, D.G., 2013. Calculation of foundation pit leakage under the condition of falling
610 bottom waterproof curtain. *Hydrogeology and engineering geology*, 40 (05): 16-21.
- 611 Gong, S.L., Ye, W.M., Chen, H.S., et al., 2008. Evaluation theory and method of ground settlement
612 of deep foundation pit engineering in Shanghai. *Chinese Journal of geological hazards and*
613 *prevention*, 19 (4): 55-60.

614 Ha, D., Zhu, K.P., Li, Z., et al., 2018. Optimization of diaphragm wall depth under confined aquifer
615 conditions in Tianjin. *Journal of underground space and engineering*, 14 (02): 490-499.

616 Li, F., Xu, J., Zhang, F., et al., 2017. Numerical simulation of uplift resistance in deep foundation
617 pit excavation under seepage. *Journal of underground space and engineering*, 13 (04): 1088-1097.

618 Li, G.M., Li, M.S., 2020. Study on dewatering control measures of foundation pit with suspended
619 waterproof curtain. *Journal of underground space and engineering*, 16 (03): 921-932.

620 Li, Y., Chen, D., Liu, X.W., et al., 2021. Simplified calculation method for decompression and
621 dewatering of deep foundation pit with suspended waterproof curtain. *Geotechnical mechanics*, (03):
622 1-8.

623 Liu, Z.Y., 2010. Study on dewatering scheme of deep foundation pit with deep and strong permeable
624 layer for Kunming Metro. *Railway Survey and design*, (5): 266-270.

625 Ni, J.C., Cheng, W.C., Ge, L., 2013. A simple data reduction method for pumping tests with tidal,
626 partial penetration, and storage effects. *Soils Found.* 53 (6), 894–902.

627 Pujades, E., De Simone, S., Carrera, J., Vázquez-Suñé, E., Jurado, A., 2017. Settlements around
628 pumping wells: analysis of influential factors and a simple calculation procedure. *J. Hydrol.* 548,
629 225–236.

630 Song, J.X., Nie, X.H., Zhang, J.Y., 2014. Prediction technology of adjacent underground pipelines
631 damage caused by excavations dewatering. *Build. Sci.* 15, 74–79 (in Chinese).

632 Tan, Y., Lu, Y., 2018. Responses of shallowly buried pipelines to adjacent deep excavations in
633 Shanghai soft ground. *J. Pipel. Syst. Eng. Pract.* ASCE 9 (2), 05018002.

634 Xu, Y.S., Ma, L., Shen, S.L., Sun, W.J., 2012. Evaluation of land subsidence by considering
635 underground structures that penetrate the aquifers of Shanghai, China. *Hydrogeol. J.* 20 (8), 1623–

636 1634.

637 Wang, J.X., Huang, T., Hu, J., 2014. Field experiments and numerical simulations of whirlpool
638 foundation pit dewatering. *Environmental earth sciences*, 71(7): 32-45.

639 Wang, J.X., Guo, T.P., Wu, L.G., et al., 2010. Mechanism and engineering application of wall well
640 interaction in deep foundation pit dewatering. *Journal of underground space and engineering*, 6 (03):
641 564-570.

642 Wang, J.X., Liu, X.T., Wu, Y, et al., 2017. Field experiment and numerical simulation of coupling
643 non-Darcy flow caused by curtain and pumping well in foundation pit dewatering. *Journal of*
644 *Hydrology*, 549: 277-293.

645 Wang, J.X., Wu, Y, Liu, X.t., et al., 2016. Areal subsidence under pumping well-curtain interaction
646 in subway foundation pit dewatering: conceptual model and numerical simulations. *Environmental*
647 *Earth Sciences*, 75(3) : 198.1-198.13.

648 Wang, J.X., Feng, B., Guo, T., 2013. Using partial penetrating wells and curtains to lower the water
649 level of confined aquifer of gravel. *Engineering geology*, 161: 16-25.

650 Wang, J.X., Hu, L, Wu, L., 2009. Hydraulic barrier function of the underground continuous concrete
651 wall in the pit of subway station and its optimization. *environmental geology*, 2009. 57(2): 447-453.

652 Wang, J.X., Feng, B., Yu, H., 2013. Numerical study of dewatering in a large deep foundation pit.
653 *Environmental earth Sciences*, 1-10.

654 Wu, Y.X., Lyu, H.M., Shen, J., Arulrajah, A., 2018. Geological and hydrogeological environment in
655 Tianjin with potential geohazards and groundwater control during excavation. *Environ. Earth Sci.*
656 77 (10), 392.

657 Wu, Y.X., Lyu, H.M., Han, J., Shen, J.S., 2019. Dewatering-induced building settlement around a

658 deep excavation in soft deposit in Tianjin, China. *J. Geotech. Geoenviron. Eng.* 145 (5), 5019003.
659 [https://doi.org/10.1061/\(ASCE\)GT.1943-5606.0002045](https://doi.org/10.1061/(ASCE)GT.1943-5606.0002045).

660 Wang, X.W., Yang, T.L., Xu, Y.S., et al., 2019. Evaluation of optimized depth of waterproof curtain
661 to mitigate negative impacts during dewatering, *Journal of Hydrology*, 577.

662 Ye, W.M., Wan, M., Chen, B., et al., 2009. Influence of dewatering in confined aquifer of deep
663 foundation pit on land subsidence. *Acta subterranean space and engineering*, (S2): 1799-1805.

664 You, Y., Yan, C.h., Liu, S., et al., 2017. Optimization design of dewatering scheme for a deep
665 foundation pit under complex geological conditions. *Acta geologica Sinica*, 25 (3): 715-722.

666 Zhao, Y.H., Tong, L.Y., Zhu, W.J., et al., 2020. Prediction and analysis of the impact of foundation
667 pit dewatering under different waterproof curtain insertion depths on the surrounding environment.
668 *Water conservancy and hydropower technology*, 51 (05): 126-131.

669 Zheng, G., Dai, X., Diao, Y., Zeng C.F., 2016. Experimental and simplified model study of the
670 development of ground settlement under hazards induced by loss of groundwater and sand. *Nat.*
671 *Hazards* 82 (3), 1869–1893.

672 Zhang, M., Fan, J., Zhao, Y.R., 2019. Study on the influence of subway station reconstruction
673 dewatering on adjacent rail transit. *Water conservancy and hydropower technology*, 50 (2): 61-68.

674

675

676

677

678

679

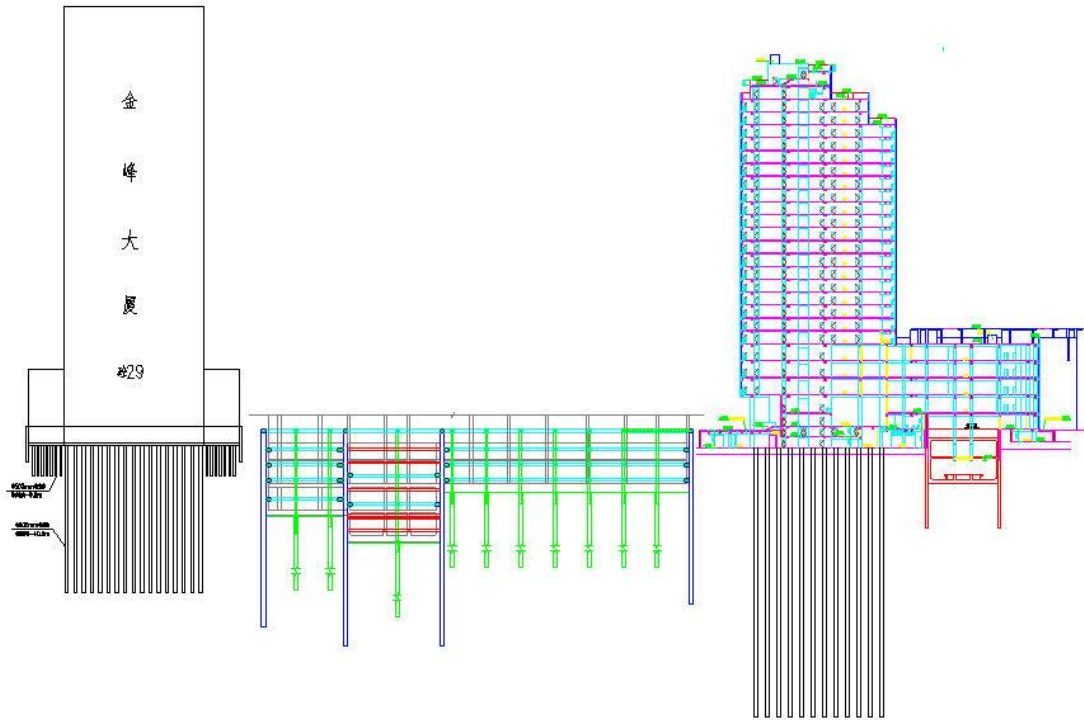
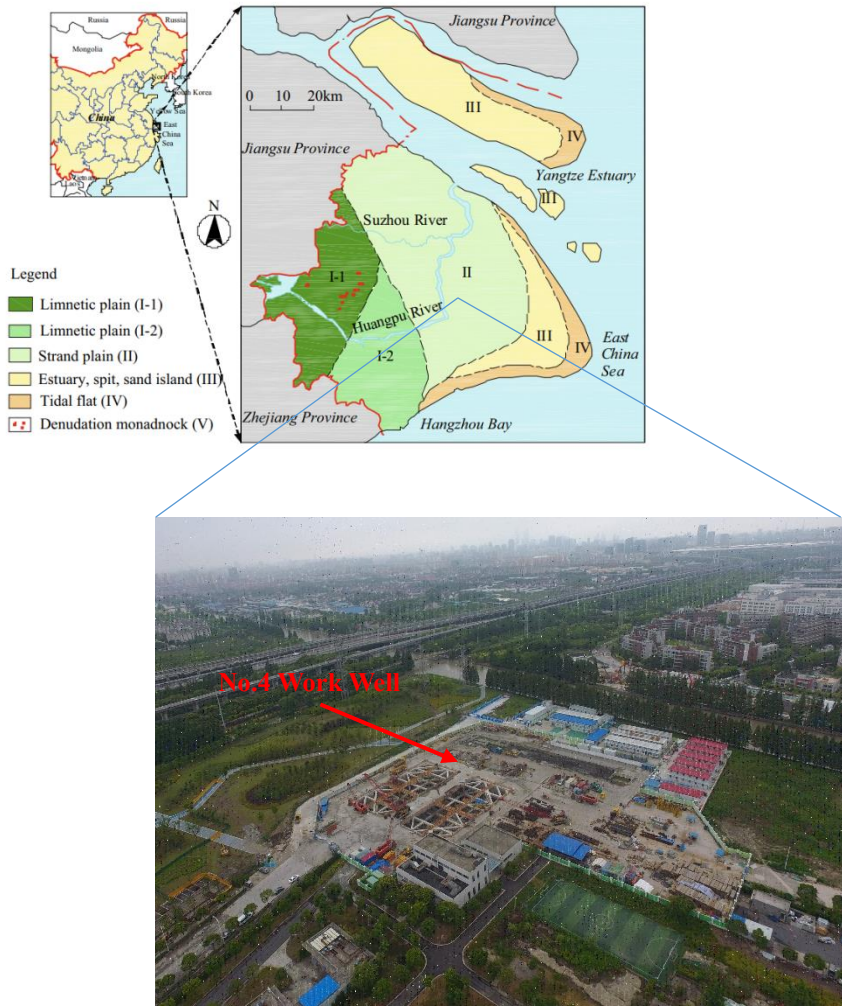
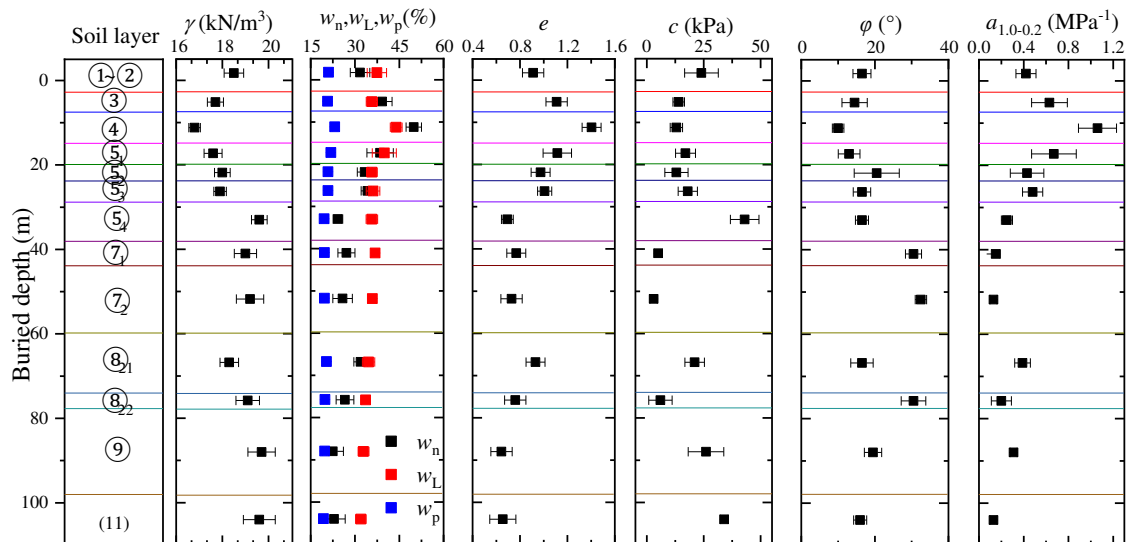


Fig. 1 Curtain cutoff, pumping and recharging measures to control groundwater level for excavation



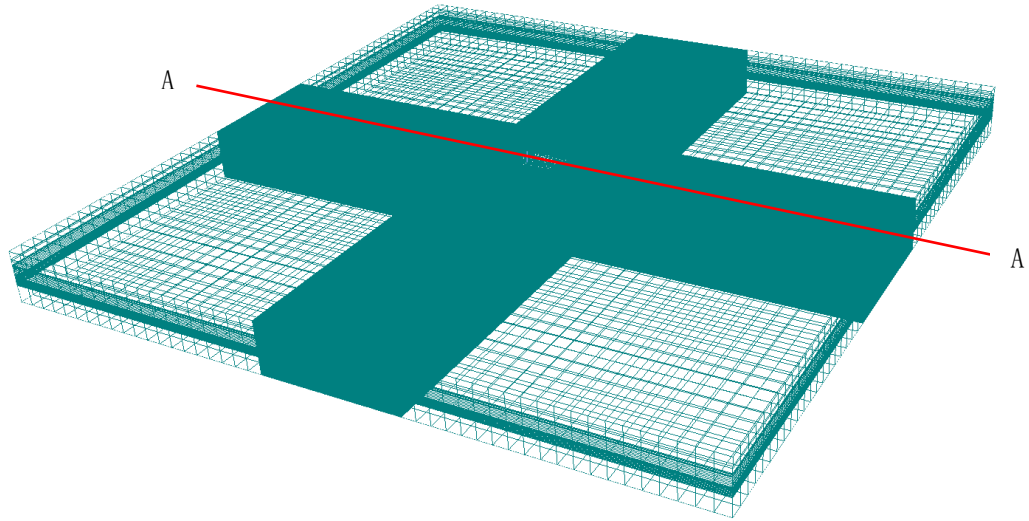
(a) Background working well base



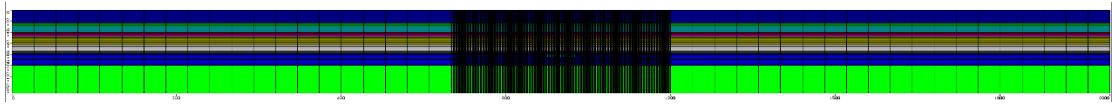
Note: γ = unit weight; w_n = water content; w_p = plastic limit; w_L = liquid limit; e = void ratio; $a_{1.0-0.2}$ = coefficient of compressibility; c = cohesion; ϕ = internal friction angle

(b) Hydrogeological Profile

Fig. 2 Layout of the No. 4 working shaft background

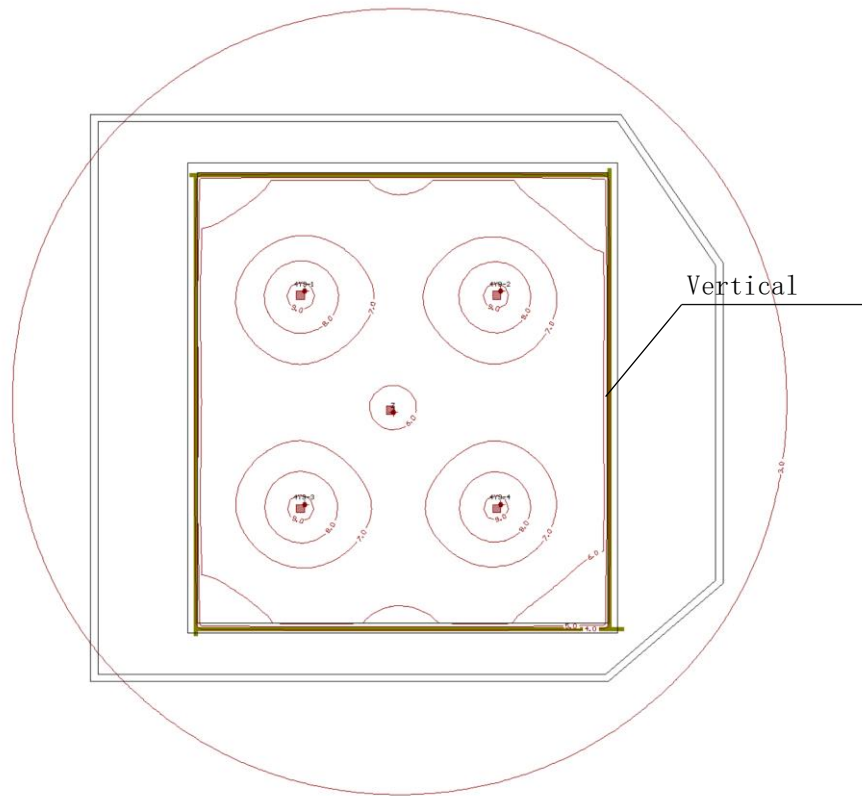


(a) 3D grid of the model

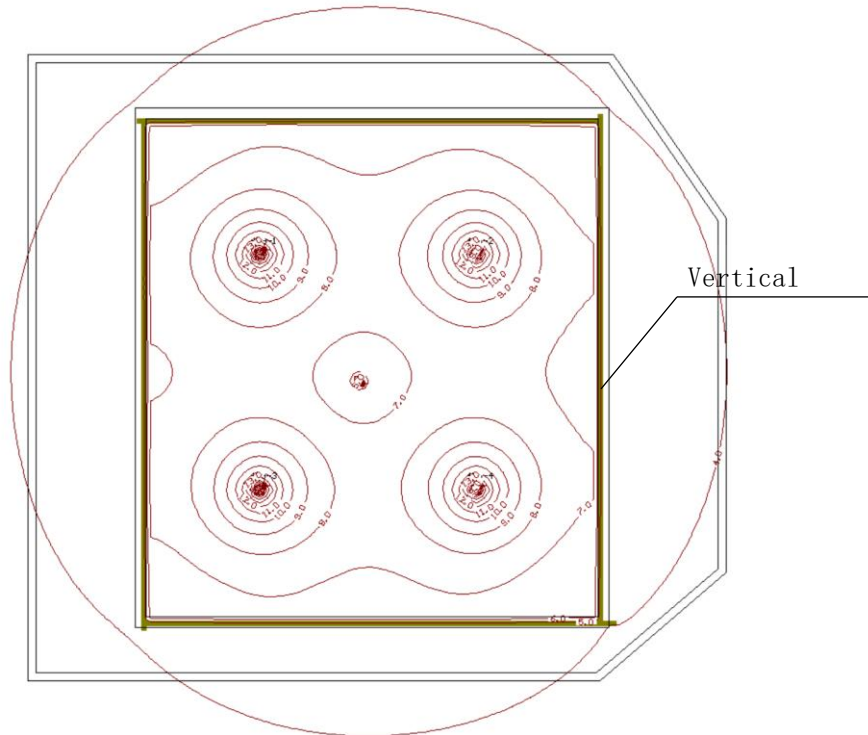


(b) Section A-A'

Fig.3 Numerical model of the MICP HSRB

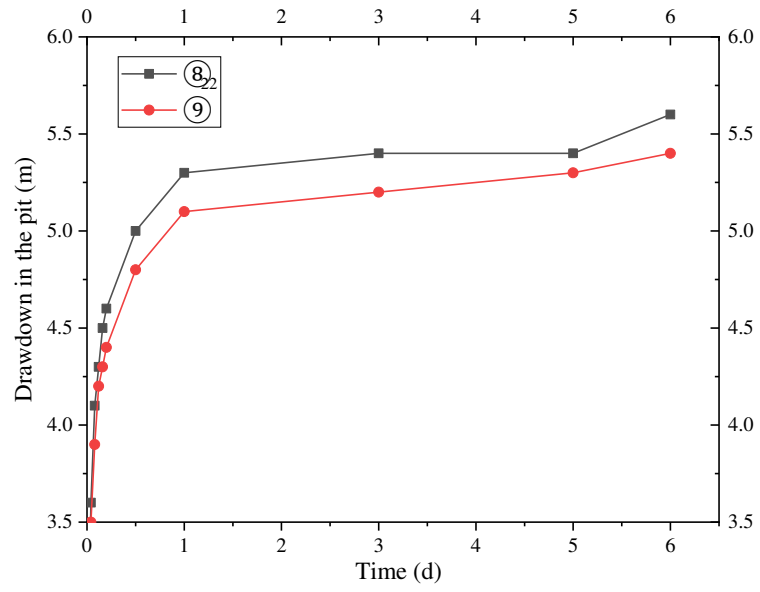


(a) Layer ②-2

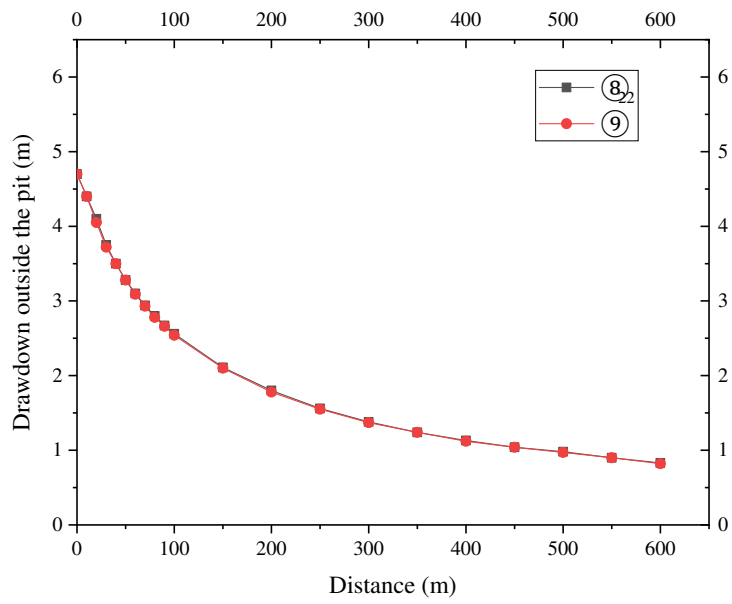


(b) Layer ⑨

Fig.4 Contour map of the aquifer drawdown



(a) Inside the pit



(b) Outside the pit

Fig. 5 Variation curve of the drawdown with distance

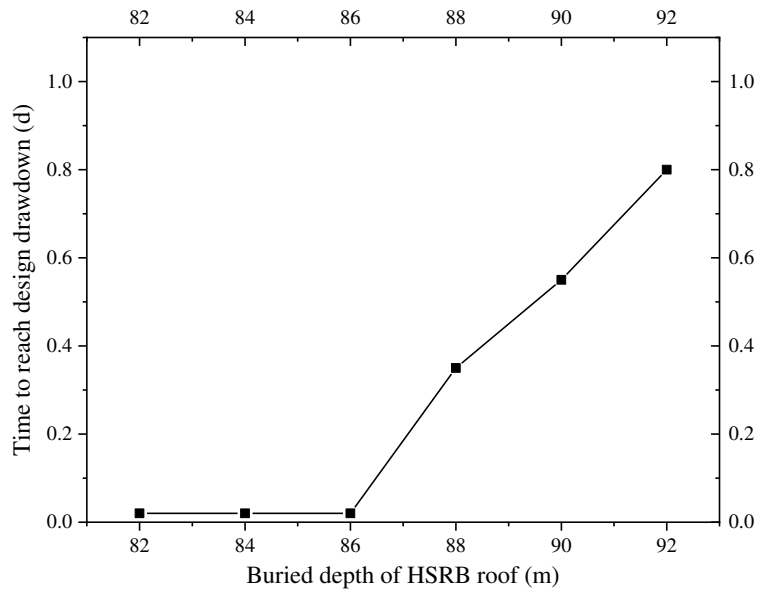
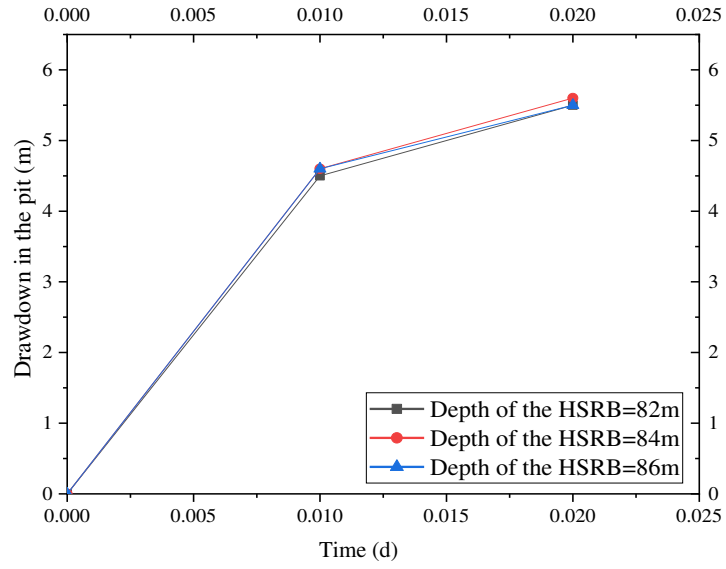
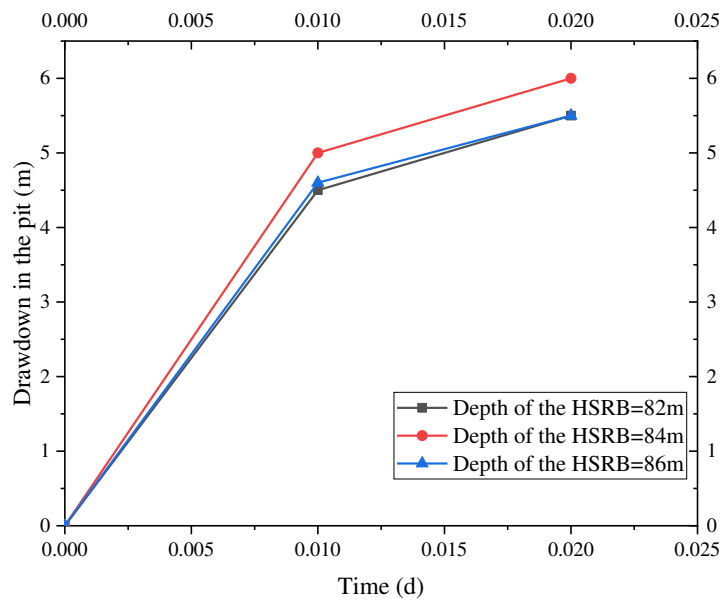


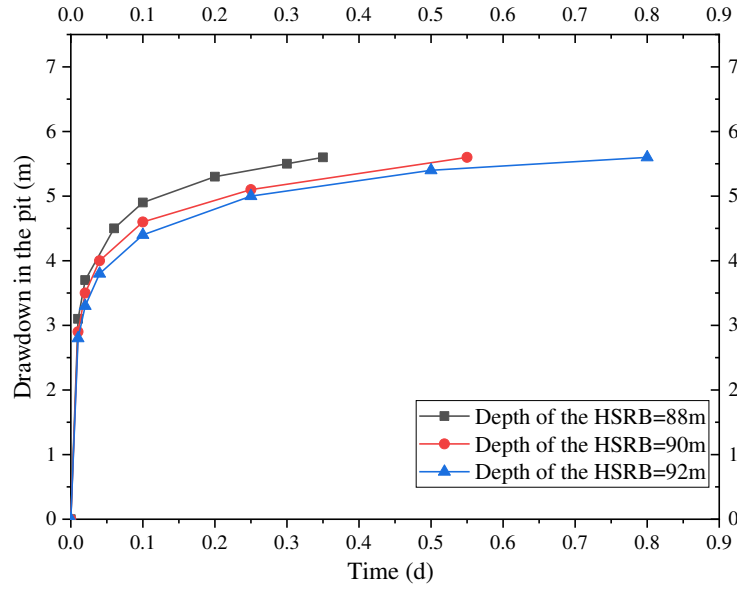
Fig.6 Time chart of the dewatering reaching the design depth of each working condition



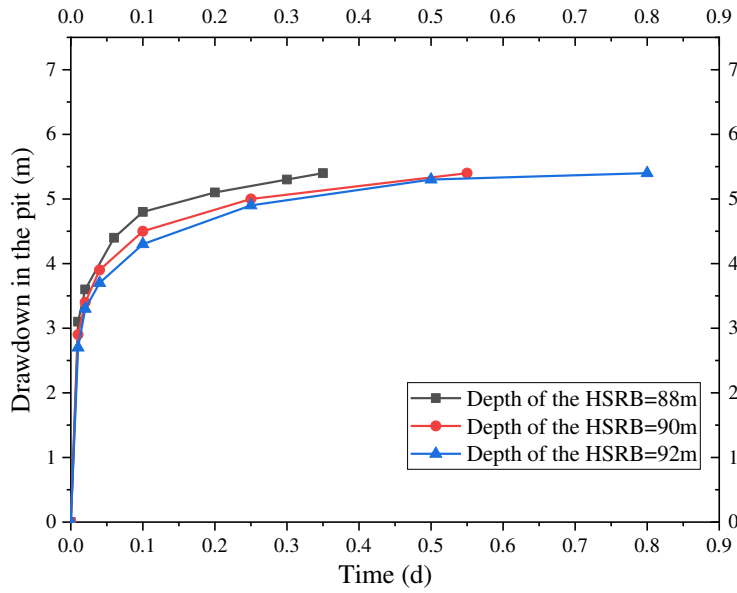
(a) Layer ②₂₂



(b) Layer ⑨

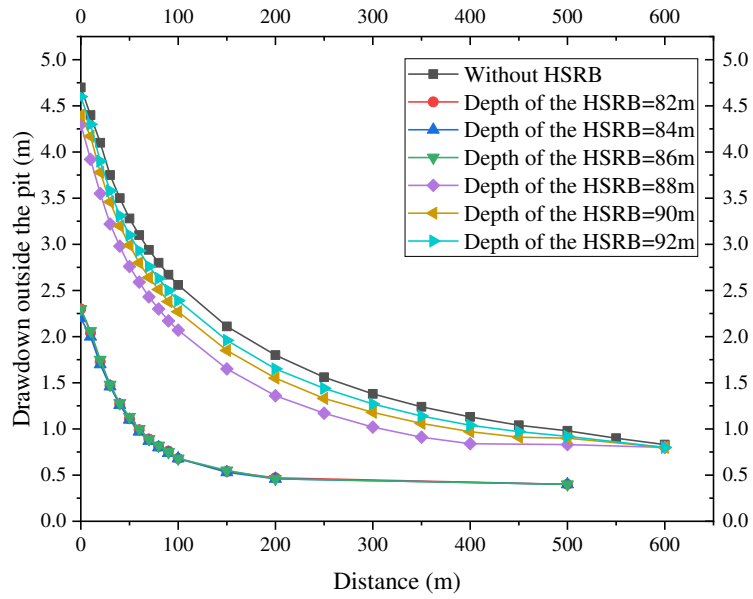


(c) Layer ⑧₂₂

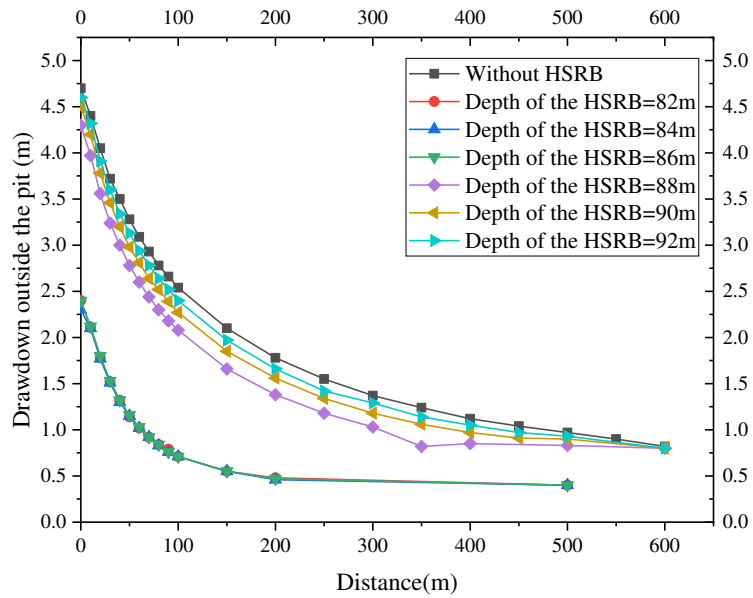


(d) Layer ⑨

Fig. 7 Drawdown-time curve in the pit with different HSRB positions

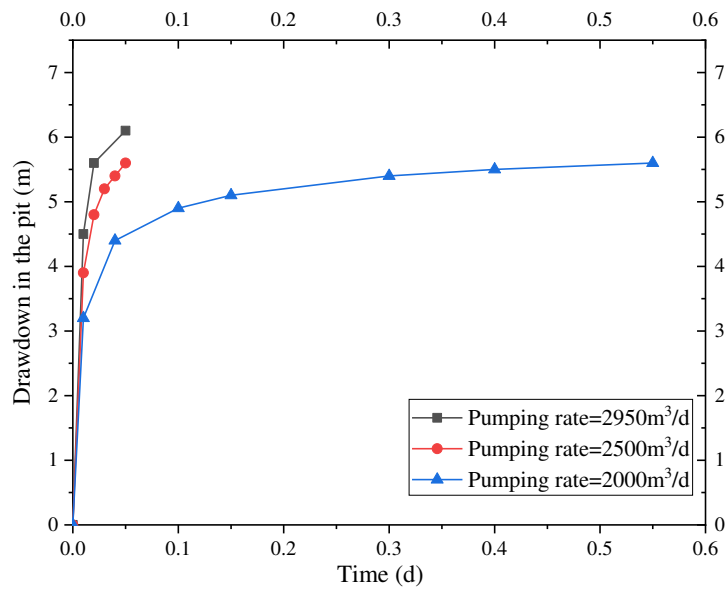


(a) Layer ⑧₂₂

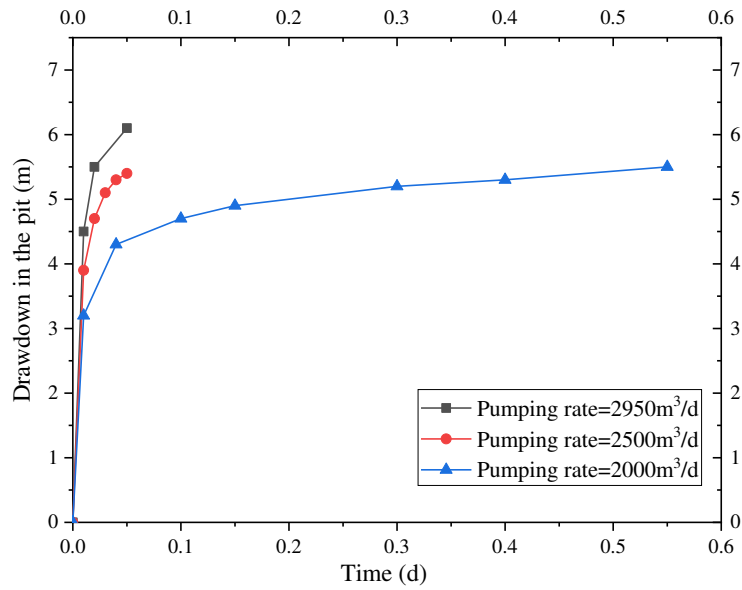


(b) Layer ⑨

Fig. 8 Drawdown-distance curve outside the pit with different HSRB positions

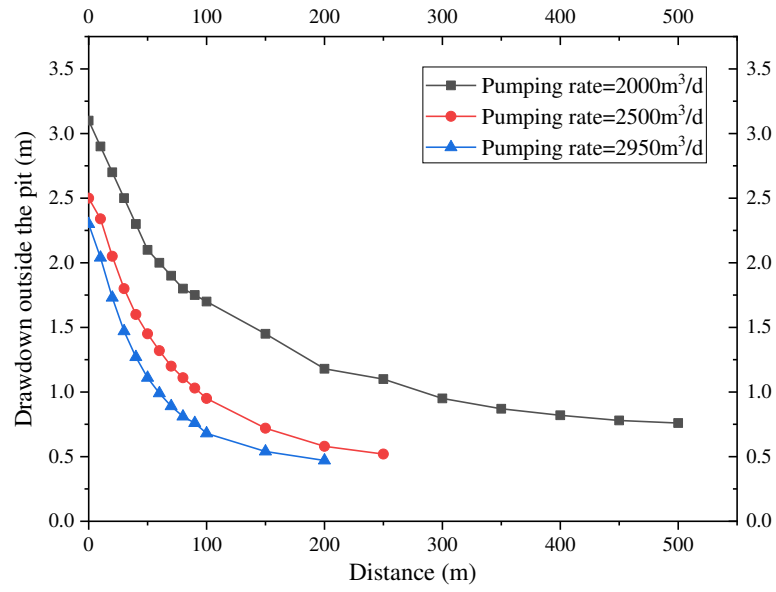


(a) Layer ②₂₂

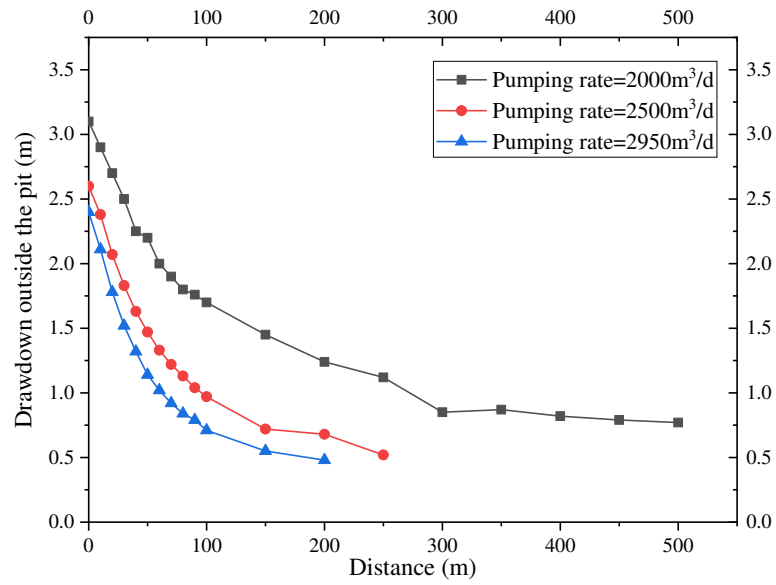


(b) Layer ⑨

Fig. 9 Drawdown-time curve in the pit with different pumping rates

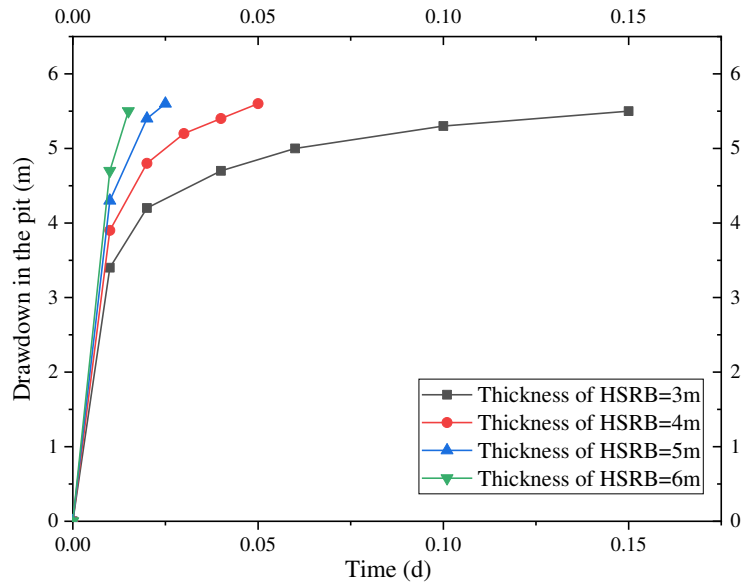


(a) Layer ⑧₂₂

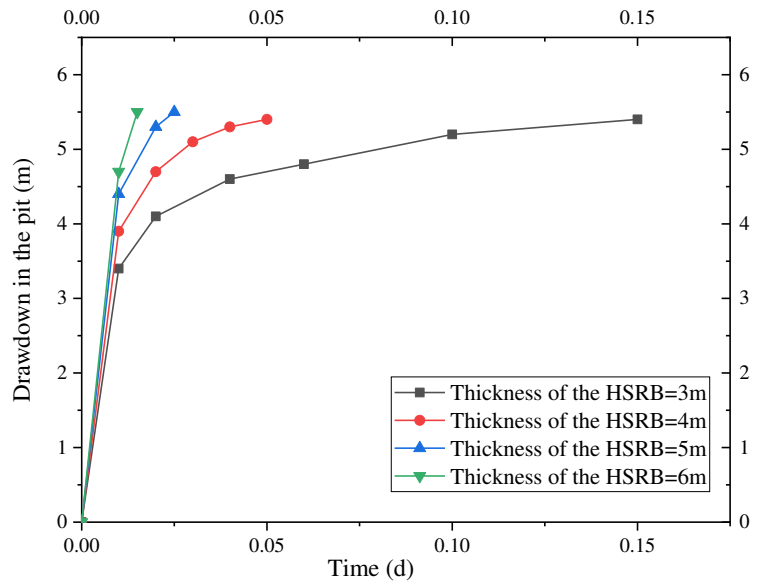


(b) Layer ⑨

Fig. 10 Drawdown-distance curve outside the pit with different pumping rates

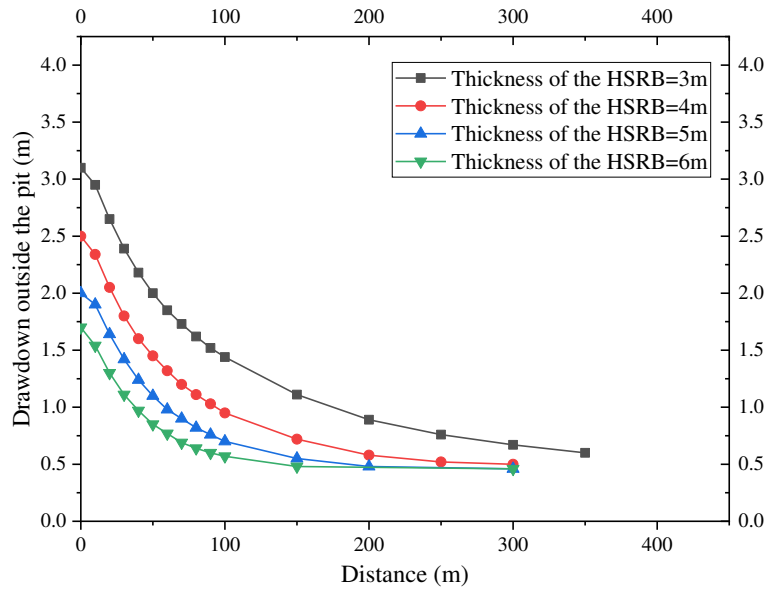


(a) Layer ⑧₂₂

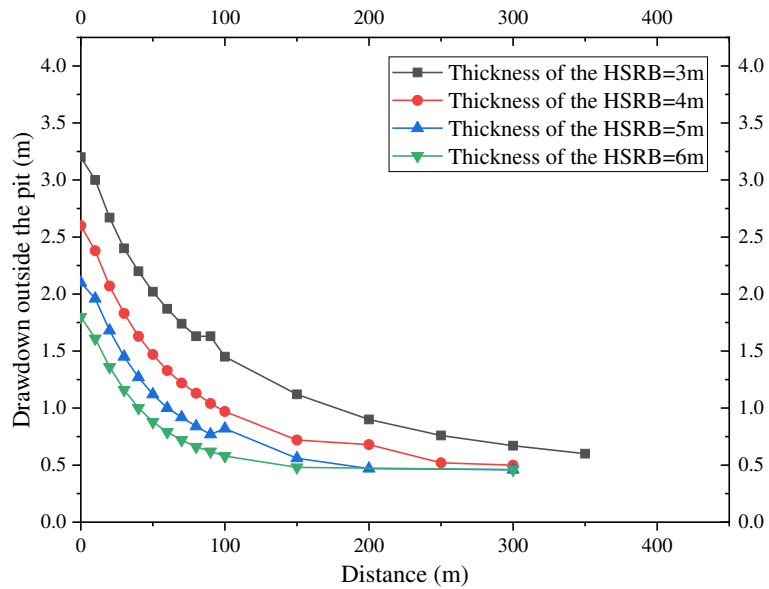


(b) Layer ⑨

Fig. 11 Drawdown-time curve in the pit with different HSRB thicknesses

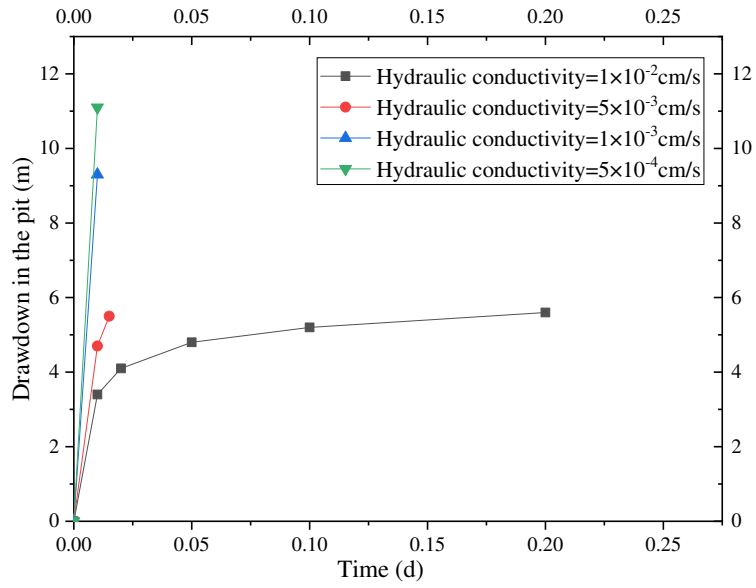


(a) Layer ⑧₂₂

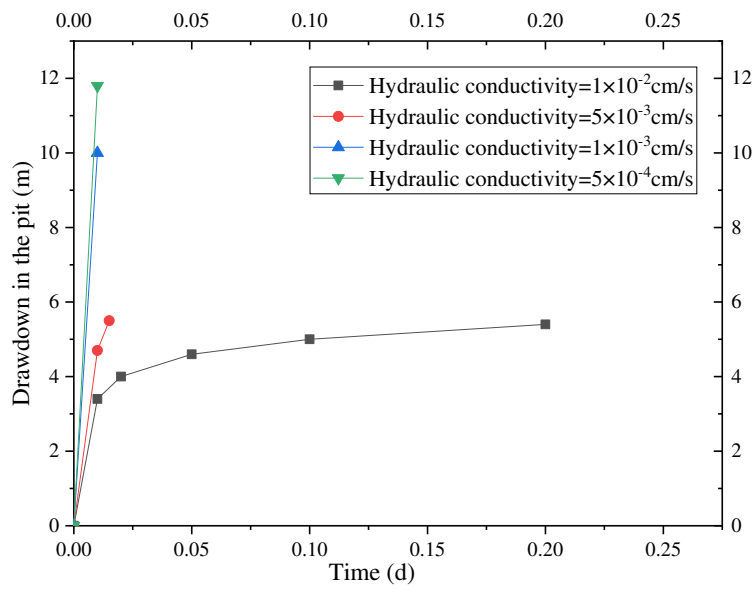


(b) Layer ⑨

Fig. 12 Drawdown-distance curve outside the pit with different HSRB thicknesses

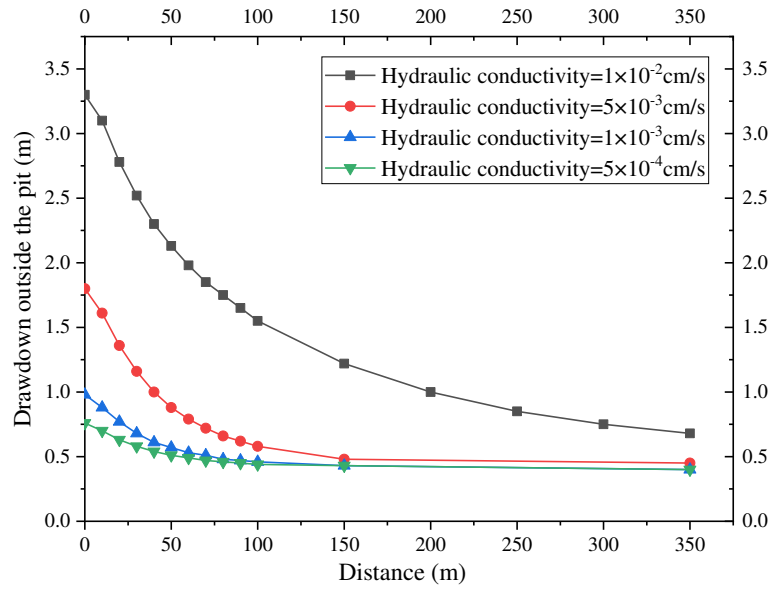


(a) Layer ⑧₂₂

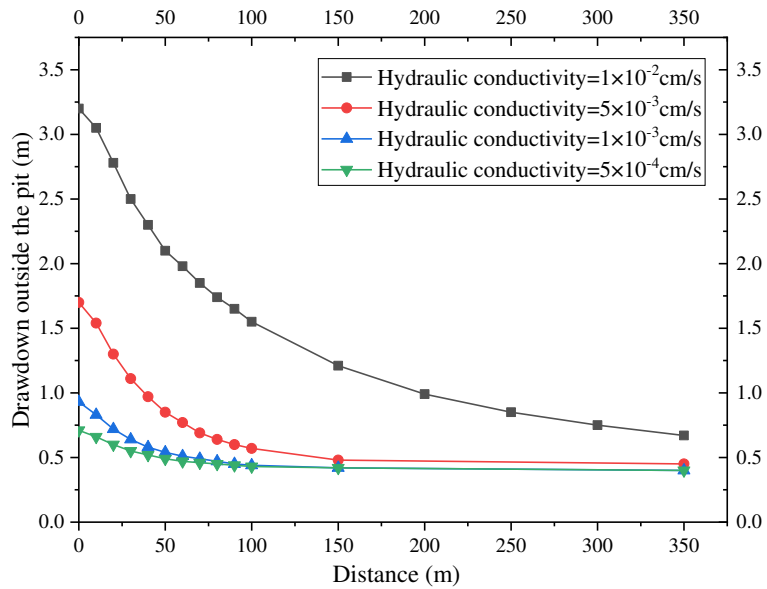


(b) Layer ⑨

Fig.13 Drawdown-time curve in the pit with different hydraulic conductivities

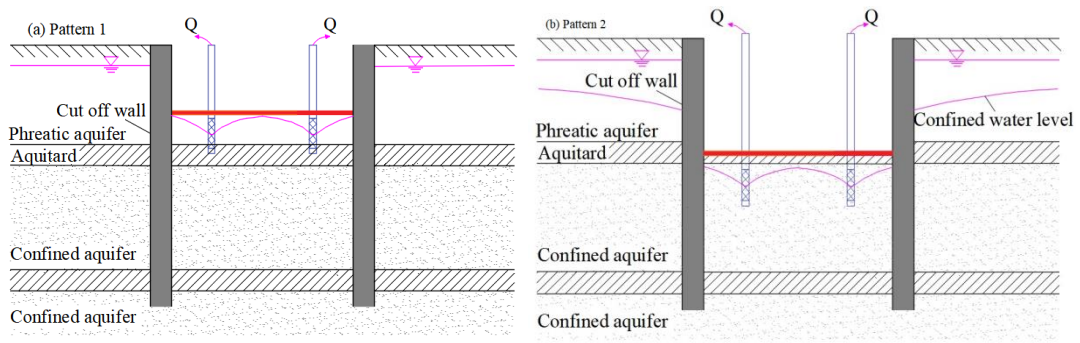


(a) Layer ⑧₂₂

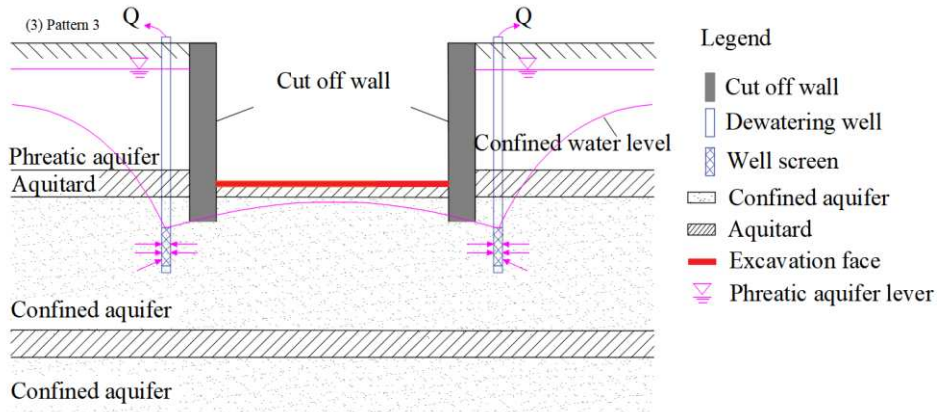


(b) Layer ⑨

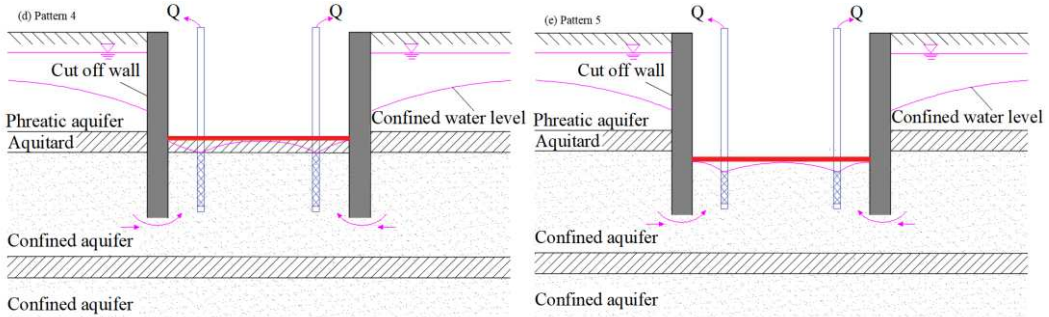
Fig. 14 Drawdown-time curve outside the pit with different hydraulic conductivities



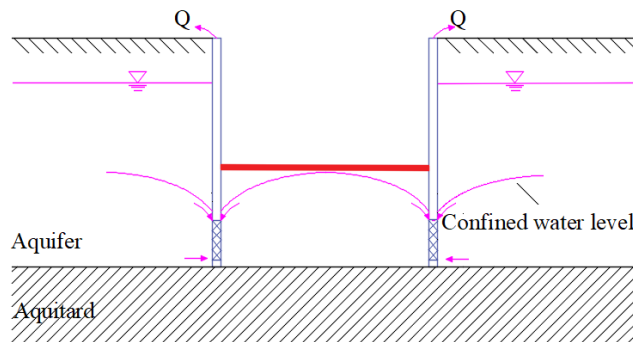
1) Mode I



2) Mode II



3) Mode III



4) Mode IV

Fig. 15 Conceptual model of four summarized seepage modes

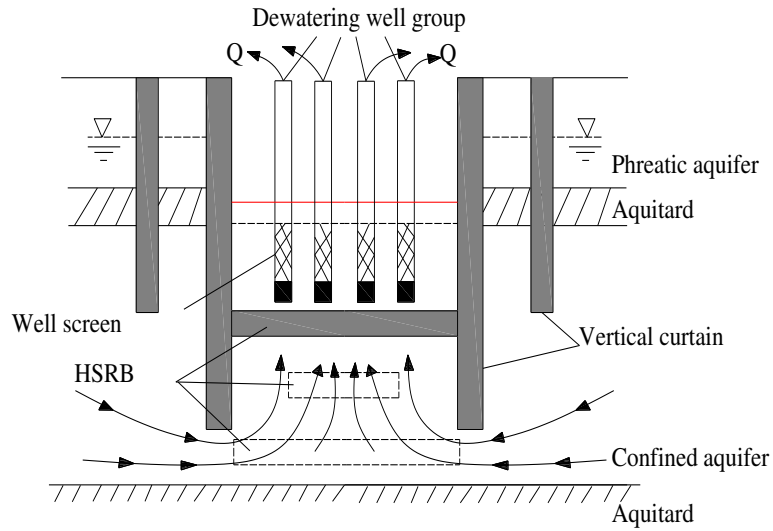
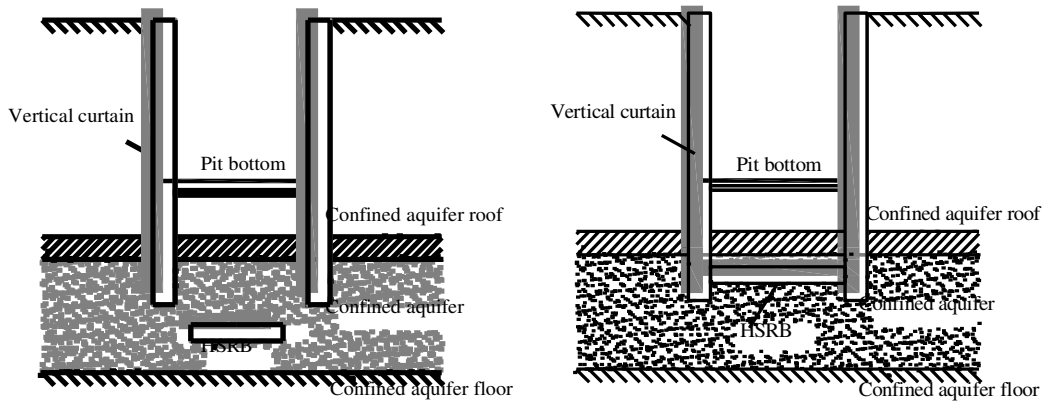
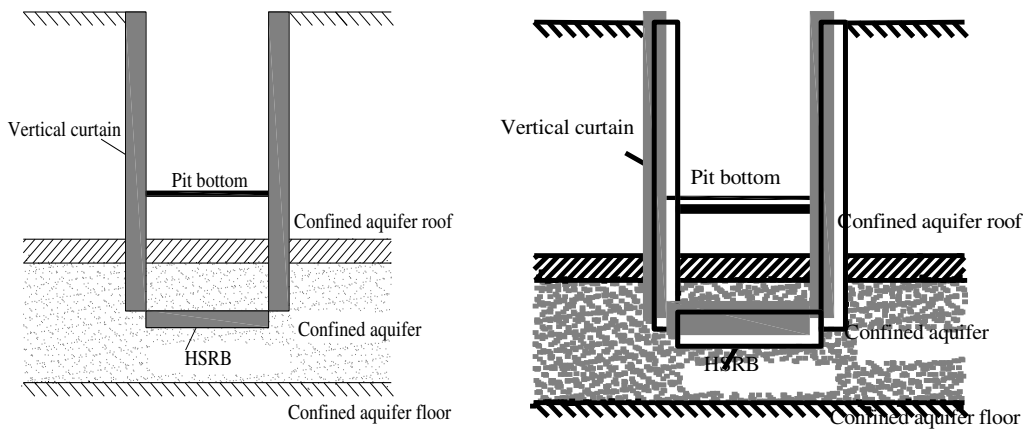


Fig. 16 Conceptual model of three-dimensional curtain-well group system



(a) V-1: Separated three-dimensional curtain (b) V-2: Inner-wrapped three-dimensional curtain



(c) V-3: Flush three-dimensional curtain (d) V-4: Transitional three-dimensional curtain

Fig. 17 Combination sub-mode of vertical curtain and HSRB

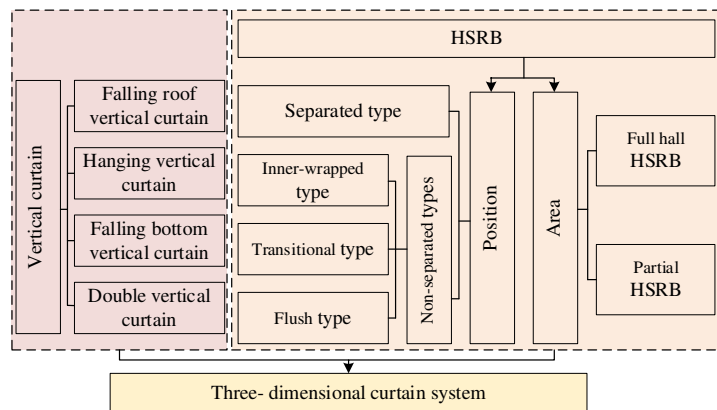


Fig. 18 Framework of the three-dimensional curtain concept system

Table 1 Hydraulic conductivity of the soil layers

Layer	Soil	Hydraulic conductivity (cm/s)	Ss (1/m)
/	Shallow clay layer	5.0×10^{-5}	8.0×10^{-4}
⑤ ₂	Clayey silt with silty clay	3.0×10^{-4}	4.5×10^{-4}
⑤ ₃	Silty clay	8.0×10^{-5}	8.0×10^{-3}
⑤ ₄	Silty clay	4.0×10^{-5}	8.0×10^{-3}
⑦ ₁	Sandy silt	1.48×10^{-3}	4.5×10^{-4}
⑦ ₂	Silt	1.40×10^{-3}	5.0×10^{-4}
⑧ ₂₁	Interlayer of silty clay and Silt	6.0×10^{-5}	4.5×10^{-4}
⑧ ₂₂	Silty sand with silty clay	6.4×10^{-3}	5.0×10^{-4}
⑨	Silt	5.0×10^{-2}	2.0×10^{-5}
(11)	Silt	1.0×10^{-2}	3.0×10^{-5}

Table 2 Statistical table for the layout of dewatering wells in foundation pit

Position	Well type	soil layers	depth	Quantity	Aperture/well diameter/well pipe thickness	Well No.	Thickness of clay ball
In pit	Dewatering well	①~⑤ ₃	38	12	650/273/4mm	4J-1~4J-12	0
	Depressurization well		68	1	650/273/6mm	4Y7-1	8m
	Depressurization well		63	1	650/273/6mm	4Y7-2	8m
	Observation well	⑦~⑧ ₂₁	60	1	650/273/6mm	4G7-1	8m
	Observation well		70	1	650/273/6mm	4G8-1	8m
	Depressurization well		85	3	850/400/8mm	4Y9-1~4Y9-3	10m
	Spare well	⑧ ₂₂ ~⑨	85	1	850/400/8mm	4YB9-1	
	Observation well		85	1	850/400/8mm	4G9-1	
Between two walls	Spare and observation well	⑤ ₂	30	4	650/273/4mm	4JG52-1~4JG52-4	0
	Spare and observation well	⑦	63	4	650/273/6mm	4JG7-1~4JG7-4	8m
Out pit	Observation well	⑦	60	4	650/273/6mm	4WG7-1~4WG7-4	8m
	Observation well	⑧ ₂₁	70	2	650/273/6mm	4WG8-1~4WG8-2	8m
	Observation well	⑧ ₂₂ ~⑨	90	1	850/325/6mm	4WG9-1	8m

Table 3 Working conditions of the influence of three-dimensional curtain on deep foundation pit dewatering

Working condition	Depth of vertical curtain (m)	Buried depth of HSRB roof (m)	Thickness of HSRB (m)	Hydraulic conductivity of HSRB (cm/s)
1		/	/	/
2		82	4	5×10^{-3}
3		84	4	5×10^{-3}
4		86	4	5×10^{-3}
5		88	4	5×10^{-3}
6		90	4	5×10^{-3}
7		92	4	5×10^{-3}
8	86	82	4	5×10^{-3}
9		82	4	5×10^{-3}
10		82	3	5×10^{-3}
11		82	5	5×10^{-3}
12		82	6	5×10^{-3}
13		82	6	1×10^{-2}
14		82	6	1×10^{-4}
15		82	6	5×10^{-4}

Table 4 Combination forms of three dimensional curtain

Working condition	Buried depth of HSRB roof (m)	Thickness of HSRB (m)	Hydraulic conductivity (cm/s)	The form of three-dimensional curtain
1	/	4	5×10^{-3}	/
2	82	4	5×10^{-3}	Inner-wrapped type
3	84	4	5×10^{-3}	Transitional type
4	86	4	5×10^{-3}	Flush type
5	88	4	5×10^{-3}	Separated type
6	90	4	5×10^{-3}	Separated type
7	92	4	5×10^{-3}	Separated type

Table 5 Working conditions of different pumping rates

Working condition	Buried depth of HSRB roof (m)	Thickness of HSRB (m)	Hydraulic conductivity of HSRB (cm/s)	Pumping rates (m ³ /d)
2	82	4	5×10^{-3}	2950
8	82	4	5×10^{-3}	2500
9	82	4	5×10^{-3}	2000

Table 6 Working conditions of different HSRB thicknesses

Working condition	Buried depth of HSRB roof (m)	Thickness of HSRB (m)	Hydraulic conductivity of HSRB (cm/s)	Pumping rates (m ³ /d)
8	82	4	5×10^{-3}	2500
10	82	3	5×10^{-3}	2500
11	82	5	5×10^{-3}	2500
12	82	6	5×10^{-3}	2500

Table 7 Working conditions of HSRB with different hydraulic conductivities

Working condition	Buried depth of HSRB roof (m)	Thickness of HSRB (m)	Hydraulic conductivity of HSRB (cm/s)	Pumping rates (m ³ /d)
13	82	6	1×10^{-2}	2500
12	82	6	5×10^{-3}	2500
14	82	6	1×10^{-3}	2500
15	82	6	5×10^{-4}	2500